1979

The effect of flow rate and canister geometry on the effectiveness of removing carbon dioxide with soda lime.

Miller, Calvin George

Monterey, California. Naval Postgraduate School

THE EFFECT OF FLOW RATE AND CANISTER GEOMETRY ON THE EFFECTIVENESS OF REMOVING CARBON DIOXIDE WITH SODA LIME

Calvin George Miller

NAVAL POSTGRADUATE SCHOOL
Monterey, California

THESIS

The Effect Of Flow Rate And Canister Geometry
On The Effectiveness Of Removing
Carbon Dioxide With
Soda Lime

by

Calvin George Miller

December 1979

Thesis Advisor: P.F. Pucci

Approved for public release; distribution unlimited.

Unclassified

SECURITY CLASSIFICATION OF THIS PAGE (When Data Entered)

REPORT DOCUMENTATION PAGE		READ INSTRUCTIONS BEFORE COMPLETING FORM
1. REPORT NUMBER	2. GOVT ACCESSION NO.	3. RECIPIENT'S CATALOG NUMBER
4. TITLE (and Subtitle) The Effect Of Flow Rate And Canister Geometry On The Effectiveness Of Removing Carbon Dioxide With Soda Lime.		5. TYPE OF REPORT & PERIOD COVERED Master's Thesis December 1979
		6. PERFORMING ORG. REPORT NUMBER
7. AUTHOR(s) Calvin George Miller		8. CONTRACT OR GRANT NUMBER(s)
9. PERFORMING ORGANIZATION NAME AND ADDRESS Naval Postgraduate School Monterey, California 93940		10. PROGRAM ELEMENT, PROJECT, TASK AREA & WORK UNIT NUMBERS
11. CONTROLLING OFFICE NAME AND ADDRESS Naval Postgraduate School Monterey, California 93940		12. REPORT DATE December 1979
		13. NUMBER OF PAGES 77
14. MONITORING AGENCY NAME & ADDRESS(if different from Controlling Office)		15. SECURITY CLASS. (of this report) Unclassified
		15a. DECLASSIFICATION/DOWNGRADING SCHEDULE

16. DISTRIBUTION STATEMENT (of this Report)

Approved for public release; distribution unlimited.

17. DISTRIBUTION STATEMENT (of the abstract entered in Block 20, if different from Report)

18. SUPPLEMENTARY NOTES

19. KEY WORDS (Continue on reverse side if necessary and identify by block number)

Carbon Dioxide Absorption
Flow Analysis
Diving System
Soda Lime
Sodasorb

20. ABSTRACT (Continue on reverse side if necessary and identify by block number)

A test installation was constructed at the Naval Postgraduate School for monitoring gas flow through a porous media bed of soda lime. The temperature, humidity, pressure and flow rates of air and carbon dioxide were controlled inputs. The exhausted fraction of carbon dioxide was measured. The ability of the soda lime in removing carbon dioxide from the incoming gas supply was determined for three cylindrical, four-inch inside-diameter

DD FORM 1 JAN 73 1473 EDITION OF 1 NOV 65 IS OBSOLETE
S/N 0102-014-6601 |
(Page 1)

Unclassified

SECURITY CLASSIFICATION OF THIS PAGE (When Data Entered)

canisters with length-to-diameter ratios of 1.225, 1.60 and 2.125, and for three steady flow rates of approximately 1, 2, and 3 SCFM. The canister was submerged in a constant-temperature water bath held at three levels: 40°F, 55°F, and 70°F. Three inlet carbon dioxide fractions of 4.0, 6.0, and 8.0 percent by volume were used. These flow rates, geometries, fractions of carbon dioxide, and temperature ranges were selected to correspond to those experienced in actual diving operations. The measure of effectiveness used in these experiments was the time of operation before the exit carbon dioxide reached one-half-percent by volume. An appropriate characteristic flow dimension and Fanning friction factor were defined by utilizing the porous media flow models of Darcy and Ward.

Approved For Public Release; Distribution Unlimited.

The Effect Of Flow Rate And Canister Geometry On The Effectiveness Of Removing Carbon Dioxide With Soda Lime

by

Calvin George Miller
Commander, United States Navy
B.S., Utah State University, 1964

Submitted in partial fulfillment of the
requirements for the degree of

MASTER OF SCIENCE IN MECHANICAL ENGINEERING

from the

NAVAL POSTGRADUATE SCHOOL
December 1979

ABSTRACT

A test installation was constructed at the Naval Postgraduate School for monitoring gas flow through a porous media bed of soda lime. The temperature, humidity, pressure and flow rates of air and carbon dioxide were controlled inputs. The exhausted fraction of carbon dioxide was measured. The ability of the soda lime in removing carbon dioxide from the incoming gas supply was determined for three cylindrical, four-inch inside-diameter canisters with length-to-diameter ratios of 1.225, 1.60 and 2.125, and for three steady flow rates of approximately 1, 2, and 3 SCFM. The canister was submerged in a constant-temperature water bath held at three levels: $40^{\circ}F$, $55^{\circ}F$, and $70^{\circ}F$. Three inlet carbon dioxide fractions of 4.0, 6.0, and 8.0 percent by volume were used. These flow rates, geometries, fractions of carbon dioxide, and temperature ranges were selected to correspond to those experienced in actual diving operations. The measure of effectiveness used in these experiments was the time of operation before the exit carbon dioxide reached one-half-percent by volume. An appropriate characteristic flow dimension and Fanning friction factor were defined by utilizing the porous media flow models of Darcy and Ward.

TABLE OF CONTENTS

LIST OF TABLES

LIST OF FIGURES

NOMENCLATURE

English Letter Symbols

a	Coefficient in Reynold's equation, the reciprical of permeability.
A_c	Canister cross sectional area.
b	Coefficient in Reynold's equation.
B	Constant in Elam's equation.
c	Dimensionless constant in Ward's equation.
D	Inside diameter of the canister.
f	Dimensionless Fanning friction factor for a porous media.
f'	Abbreviated representation of the dimensionless Fanning friction factor for a porous media.
k	Permeability of a porous media.
$\sqrt{k}$	Characteristic flow dimension.
L	Length of the Sodasorb bed in the canister.
$\dot{m}$	Mass flow rate.
P	Pressure.
Q	Volumetric flow rate.
R	Gas constant.
Re	Reynolds number.
$t_{1/2}$	Time to reach 0.5% carbon dioxide by volume in the exhaust gas of the canister. A measure of effectiveness of absorbents.
V_c	Macroscopic, superficial, filtration velocity of a porous media.
x	Distance measured from the incoming gas screen along the length of the canister.

Greek Letter Symbols

Δ	Difference or change.
μ	Fluid viscosity.
ρ	Fluid density.

Subscripts

atm	Local atmosphere.
c	Canister.
f	Flowmeter.
L	Length of the Sodasorb bed.
s	Standard (temperature and pressure).

ACKNOWLEDGEMENT

The author would like to express his appreciation to Dr. Paul F. Pucci, Professor of Mechanical Engineering, for his leadership, patience and technical assistance.

The skilled craftsmen Messrs. T. Christian, K. Mothersell, "Junior" Dames and R. Longueira were instrumental in developing apparatus with which to conduct this experimental investigation.

The financial and technical support of the Naval Coastal Systems Laboratory, Panama City, Florida is gratefully acknowledged. NARF, North Island Naval Air Station personnel were instrumental in providing carbon dioxide measurement equipment and training. Their loan of the infrared detector to the Naval Postgraduate School was appreciated.

The assistance provided by Dr. Robert H. Nunn, Associate Professor of Mechanical Engineering, in taking time to review and return beneficial suggestions on the rough drafts of this thesis was appreciated.

I. INTRODUCTION

As the state-of-the art in deep sea diving has progressed, the need of recirculation of the diver's expelled breath was required to increase the dive duration and reduce the size, volume and cost of the breathing gas supply, particularly in self contained systems. Recirculation conserves the inert gas, nitrogen or helium, and thus only the required make-up of oxygen is replenished. The carbon dioxide produced by the diver must be removed from the expelled breath. An excessive amount of carbon dioxide in an incoming breath may cause an increase in the breathing rate, or without warning may cause unconsciousness.

For a volume of oxygen consumed, slightly less than that volume of carbon dioxide is expelled [1][1]. The amount of oxygen consumed varies by a factor in excess of two between complete rest and exhaustive work.

Lime water was used as early as the eighteenth century for removing carbon dioxide from gas mixtures. The early attempts to remove carbon dioxide from a person's expelled breath was by the medical profession. In 1842 two American physicians employed diethyl ether to produce complete anesthesia. This diethyl ether created an explosive atmosphere, and provided anesthesia to the physician as well as to the

---

[1] Numbers in brackets refer to items in the bibliography.

patient. Mine rescue apparatus were used a few years later with an alkali unit to remove carbon dioxide.

H.A. Fleuss [1] a British diver utilized a workable solution of caustic potash in 1878 to remove carbon dioxide in a rebreathing self-contained underwater apparatus. In 1927 the U.S. Navy commenced investigation of diving deeper than air mixtures would safely allow by utilizing breathing mixtures of helium and oxygen. The storage space required and the expense of these mixtures necessitated minimizing the gas supply for supporting a diver by recirculating his expelled breath through a carbon dioxide removing canister attached to the existing deep diving suit. This system was successfully utilized to rescue submariners from the stricken submarine SQUALUS in 1939.

Sodasorb [2] is a registered trademark name for Wilson Soda Lime used by the Allied armies in a gas mask near the end of World War I and utilized today in diving. High performance (HP) Sodasorb consists of calcium hydroxide, 14 to 19 percent moisture by weight, less than three-percent sodium hydroxide or potassium hydroxide, ethyl violet as a sensitive acid base indicator, and minor quantities of barium hydroxide. The void space between particles in a bed of Sodasorb is approximately 47 percent of the gross volume. The removal of carbon dioxide by Sodasorb is a chemical reaction. The carbon dioxide forms carbonic acid which combines with hydroxide to form sodium carbonate and water. Some of the sodium carbonate then reacts with lime to form calcium carbonate. This process may be expressed by the following equations:

$$CO_2 + H_2O \rightleftharpoons H_2CO_3$$

$$2H_2CO_3 + 2Na^+ + 2OH^- + 2K + 2OH^- \rightarrow$$

$$2Na^+ + CO_3^= + 2K^+ + CO_3^= + 4H_2O$$

$$Ca(OH)_2 + H_2O \rightleftharpoons Ca^{++} + 2OH^- + H_2O$$

$$2Ca^{++} + 4OH^- + 2Na^+ + CO_3^= + 2K^+ + CO_3^= \rightleftharpoons$$

$$2CaCO_3 + 2Na^+ + 2OH^- + 2K^+ + 2OH^-$$

Ideally, at atmospheric pressure, one cubic foot of Sodasorb could remove as much as 200 cubic feet of carbon dioxide. The Federal Caustic Poison Act limits the maximum content of NaOH and/or KOH to ten percent; however, only about three percent is considered safe to be included in Sodasorb. Above three percent, the rate of carbon dioxide removal is thought to decrease.

Carbon dioxide removal is necessary in hyperbaric chambers, mixed-gas surface-supplied diving suits, long-duration compact self-contained free swimming diving suits and in submarine atmospheric environments. In 1968 personnel of the Navy Experimental Diving Unit carried out tests in the techniques of remaining at depths in excess of 800 feet for extended periods of time without apparent adverse effects. These "saturation" tests supplied the necessary equipment and technical knowledge for the establishment of operational Deep Dive Systems that have vastly extended the diving capability to depths exceeding 1000 feet in the open sea while

utilizing various carbon dioxide removing apparatuses. The time limitation of dives utilizing carbon dioxide removal systems is dependent upon the effectiveness of the absorbent to remove the carbon dioxide.

An adequate fresh quantity of Sodasorb will remove all the carbon dioxide initially expelled by a diver. As time goes on, more carbon dioxide passes through the Sodasorb and when the level of carbon dioxide recirculated to the inlet breath exceeds one-half of one-percent by volume, it is considered to be a health hazard. This is the limit imposed on the exit percentage of carbon dioxide, even though the absorbent is still capable of removing more carbon dioxide. The measure of effectiveness of a given absorption system is therefore the maximum permissible time of operation before the exit carbon dioxide reaches a half-percent by volume.

Consideration must be given to the pressure drop across a bed of absorbent as well as to the effectiveness of that absorbent. The pressure drop across the absorbent must be limited to provide ease in breathing for the diver. Therefore, the pressure drop characteristics of the absorbent must be known in determining the most effective absorption system design.

The Navy Experimental Diving Unit and the Naval Coastal Systems Laboratory in Panama City, Florida are actively engaged in a Navy diving improvement program. Numerous tests have been conducted on modified canisters using both man breathing and simulated breathing apparatus.

This thesis research has been an initial attempt in an overall program to more-completely understand the behavior of carbon dioxide absorption by Sodasorb. In particular the objectives were:

1. Construct a test installation for measuring gas flow through a canister, the volume percentage of carbon dioxide into and out of the canister, the temperatures and pressures inside the canister while controlling humidity, the temperature of the incoming gas supply and the canister environmental temperature.
2. Determine the appropriate characteristic flow dimension to be used in the Reynolds number for correlating the flow friction characteristics of Sodasorb.
3. Determine the effect of flow rate and flow geometry of a cylindrical canister on the effectiveness of Sodasorb in removing carbon dioxide.

II. SUMMARY OF THEORY

A. FLOW IN A POROUS MEDIA

The general treatment of percolation through soils-utilized by hydraulic engineers in sanitary installations, soil formations beneath hydraulic structures and in the materials of the structure themselves-has application in analyzing fluid flow through Sodasorb. The voids in a matrix of Sodasorb form numerous small channels that are varying in shape and are complex in nature.

In 1856, Darcy [3] conducted flow experiments on sand filters. These experiments provide the basis for theory of flow of homogeneous fluids through porous media. His results were simply that the rate of flow through the porous media was directly proportional to the area of the sand and the difference between the pressure head at the inlet and outlet, and inversely proportional to the length of the bed. Darcy's law for laminar flow in a porous media is

$$-dp/dx = \mu V_c/k \qquad (1)$$

where dp/dx is the pressure gradient in the flow direction, k is the permeability of the porous media, μ is the absolute viscosity of the fluid passing through the porous media and V_c is the macroscopic velocity defined by:

$$V_c = Q/A_c \qquad (2)$$

where:

Q = volumetric flow rate

A_c = Cross sectional area of the media.

This velocity is referred to as the superficial velocity by Beavers and Sparrow [4], filtration velocity by Scheidegger [5] and macroscopic velocity by Muskat [3] and Ward [6].

Reynolds and later Muskat [4] suggest that for flow beyond the range of laminar flow the axial pressure gradient should be represented by the form

$$-\frac{dp}{dx} = a\mu V_c + b\rho V_c^2 \tag{3}$$

where a and b are constants of the media and ρ is the density of the fluid passing through the media. It is expected that, due to the tortuous and irregular channels, the transition between laminar and turbulent types of flow will not be as sharp as in pipe flow or flow over a flat plate. Beavers and Sparrow emphasize that non-Darcy flows are not necessarily turbulent. An initial departure from the slower flow is due to separation and wake effects (inertia effects) which are due to shear forces alone increasing the pressure gradient.

It can be seen for very slow flow that the first term in non-Darcy flow must be equal to the terms in Darcy's law. Thus 'a' equals the inverse of permeability. Dividing the non-Darcy flow equation by μV_c provides the form

$$\frac{1}{\mu V_c}\left(-\frac{dp}{dx}\right) = \frac{1}{k} + b\,\frac{\rho V_c}{\mu} \tag{3a}$$

Rearranging into the familiar form of $y = bx + c_1$ gives:

$$\frac{1}{\mu V_c}\left(-\frac{dp}{dx}\right) = \left(\frac{\rho V_c}{\mu}\right) b + \frac{1}{k} \tag{3b}$$

The data of Beavers and Sparrow confirmed the experimental results of Ward in this relationship between axial pressure gradient and flow rate. From the plot of experimental data, the vertical intercept yields the reciprical of permeability and the slope of the line yields the parameter b. Ward employed dimensional analysis in an attempt to unify the flow friction parameters for all porous media of a similar structure. His results employ the square-root of permeability as a characteristic flow dimension and define the Fanning friction factor for a porous media. In addition to Ward's experimental results, Beavers and Sparrow, in experiments with fibrous porous media, lend support to the use of the square-root of permeability as the characteristic dimension in the definition of the Reynolds number and to this same definition for a Fanning friction factor in porous media.

Employing the square-root of the permeability as a characteristic flow dimension the Reynolds number and Fanning friction factor for a porous media are defined by:

$$Re = \frac{\rho V_c \sqrt{k}}{\mu} \tag{4}$$

$$f = \frac{-dp}{dx} \frac{\sqrt{k}}{\rho V_c^2} \tag{5}$$

$$f' = \frac{1}{Re} + c \tag{5a}$$

$$c = \sqrt{k}\ b \tag{6}$$

B. CARBON DIOXIDE REMOVAL

Documented research in evaluating the effectiveness of Sodasorb has been primarily oriented to anesthesia. Anesthetic use of the absorbent differs from the undersea use of the absorbent primarily in that the diver exposes the canister to increased pressures, gas flow rates, fractions of carbon dioxide, and to decreased temperatures.

Adriani and Byrd [7] analytically determined that optimum effectiveness is obtained when the air space of the absorbent is equal to or greater than the tidal volume[2] of the patient. Conroy and Seevers [8], concluded that one baffle plate should be utilized for improved efficiency in a to-and-fro[3] anesthesia canister. At temperatures in excess of 70°F, Conroy and Seevers results indicate that effectiveness was not changed by altering temperatures. Ten Pas, Brown and Elam [9], compared the advantages of the to-and-fro system with those of the circle system[4]. They concluded that the intermittent use of soda lime did not appreciably increase its capability to remove carbon dioxide.

---

[2] Tidal volume is the volume of gas exhaled per breath.

[3] A to-and-fro system places the canister near the patient's mouth and the gas travels through the same tube in flowing to and from the canister.

[4] A circle system consists of a loop in which the gas is allowed to travel in only one direction.

In addition to the effectiveness of the absorbent to absorb carbon dioxide, the pressure drop across the absorbent must be limited to insure ease of breathing. Therefore, the pressure-drop characteristics of the absorbent are required for the most effective absorption system design. In an investigation by Elam [10] of a bed of Sodasorb of length, L, cross sectional area, A, the flow resistance, ΔP, with a gas velocity, V, is given by:

$$\Delta P = \frac{B\ L\ Q}{A} \quad \text{where} \quad B \approx \frac{.0366 \text{ inches of water min}}{\text{ft}^2} \qquad (7)$$

Elam recommends that in anesthesia applications a simple cylindrical canister be used with an air distributor at the inlet and, to avert channeling at the wall of the compartment, annular rings should be installed at intervals along the wall.

Brown [11] deduced that the fraction of carbon dioxide remaining in the gas should, in theory, decrease logarithmically along the length of the canister.

The manufacturers of Sodasorb define a "break point" or time-efficiency which is the number of minutes of continuous use under standard anesthesia conditions before the patient begins to receive the first traces of his own carbon dioxide. This is as a measure of the absorption efficiency and capacity [2].

The performance factor utilized in this experimentation is the time a given absorption system operates before the exit carbon dioxide reaches one-half percent by volume. This

measure of effectiveness of Sodasorb is used throughout this experimentation and is easier identified and more quantitative than the "first traces".

The amount of carbon dioxide absorbed in the canister cannot be measured directly. The percentage-by-volume of carbon dioxide leaving the canister can be measured directly.

A correlation of steady flow rates to unsteady flow rates is necessary to relate the results of this experimentation with the conditions affecting a diver breathing through a canister. Some reliable source of information on flow rate variations with time in a specific diving system must first be obtained and this information is not presently available. Most diving systems have inhalation and/or exhalation bags before and/or after the canister. These flexible bags and the total volume of gas in the system provide some damping of the diver's breathing signature prior to the gas entering the canister. In any case, correlation of steady flow rates to unsteady flow rates was not attempted in this investigation.

The ability of the Sodasorb in removing carbon dioxide from the incoming gas supply was determined for three cylindrical canisters, four-inch inside-diameter, with length-to-diameter ratios of 1.225, 1.60 and 2.125, and for three steady flow rates of approximately 1, 2 and 3 SCFM. The canister was submerged in a constant-temperature water bath held at three levels: $40^{\circ}F$, $55^{\circ}F$, and $70^{\circ}F$. An input percentage-by-volume of carbon dioxide of 6.0 percent was used

in all cases and, in addition, 4.0% and 8.0% was used at the 2 SCFM flow rate.

III. EXPERIMENTAL APPARATUS

A primary objective was to construct a test installation for measuring gas flow through the canister, the volume percentage of carbon dioxide into and out of the canister, the temperatures and pressures inside the canister while controlling humidity, the temperature of the incoming gas supply, and the canister environmental temperature. The overall system schematic is shown in Figure 1. The following system description is divided into five subsystems: gas supply and flow measurement, carbon dioxide measurement, temperature measurement and control, description of the canister, and pressure measurements within the canister.

A. GAS SUPPLY AND FLOW MEASUREMENT

An Ingersol-Rand three-stage low-pressure 40 horsepower air compressor (shown in Figure 2) was utilized to charge two air banks to 190 psig. The air was filtered and cooled prior to storage in the air banks. A Fairchild Hiller Model 10 air regulator reduced the air pressure to ten psig. The flow rate of air was then controlled by a 3/8-inch gate valve and filtered through a ten micron filter.

The medical grade carbon dioxide was supplied in high pressure cylinders reduced to ten psig by a Matheson Model 8-320 regulator. The carbon dioxide was piped to a Hoke control valve and then admitted to the main air supply line.

The mixture of carbon dioxide and air passed through a half-inch Fischer and Porter Model 10A3500 convertible indicating flowrator meter (shown in Figure 3) rated at 4.6 standard cubic feet per minute at a standard temperature of 70°F and standard pressure of 14.7 psia [12]. The main gas supply line then contained a thermocouple, 1/2-inch gate bypass-valve, 1/2-inch gate supply-valve, tap cutoff for measuring $P_f - P_{atm}$ and a carbon dioxide tap cutoff. $P_f - P_{atm}$ was measured with a Meriam Type W 0-30 inches of mercury manometer.

After the supply valve, the gas passed through a 1/2-inch Model FT-4-8N25-GB Flow Technology standard line flowmeter (shown in Figure 3). This turbine meter was calibrated from 0.3 to 2.6 cubic feet per minute. The output of the turbine meter was fed to an electronic signal conditioning circuit in a 1950-A Fluke digital frequency counter (set at a maximum cycle rate and 10 seconds summation counting period). The output frequency (Hz) was converted linearly to flow rate from the manufacturer's gas flow calibration data sheets. After the turbine meter the gas passed by a thermocouple and a tap cutoff for measuring $P_f - P_{atm}$ with a Meriam type W 0-30 inches of mercury manometer. The gas was then piped to the water bath.

For resistance-to-flow measurements with nitrogen, the nitrogen was piped through the carbon dioxide line.

During the carbon dioxide effectiveness experimentation and when using humid air while measuring flow resistance, the gas was piped into the water bath first-stage copper-cooling-coils, first-stage humidifier, second-stage cooling-coils, second-stage humidifier, primary water-separator (shown in Figure 4) and then to the canister.

Prior to entering the canister the gas passed by a tap cutoff which led to the infrared detector for monitoring the volume-percentage of carbon dioxide.

B. CARBON DIOXIDE MEASUREMENT

Carbon dioxide was measured with a modified Wilks Miran IA (shown in Figure 3) variable filter infrared analyzer. The incoming continuous flow of gas was dehumidified by passing it through a bed of anhydrous indicating Drierite ($CaSO_4$). The incoming gas to the infrared detector was at $70^{\circ}F$ and atmospheric pressure. The infrared detector was calibrated prior-to and upon completion of each run with nitrogen, 0.5%, 1.0%, 4.0%, 6.0% and 8.0% by volume carbon dioxide and pre-mixed nitrogen. These calibration gases were available through a distribution manifold with air quick-disconnects.

Prior to each run the canister input gas was sampled from the rotameter exhaust tap. After termination of each run the input gas was sampled from the rotameter exhaust tap and the canister input tap. These samples were compared to the desired calibration nitrogen and carbon dioxide premixed gases. The infrared detector was utilized in an open loop mode at a wavelength of 4.25 micrometers, slit of 2 millimeters,

gain of 10, and the continuous gain was fine-tuned to a meter reading of zero with nitrogen purging the test cell. The time constant on the infrared detector was one second, the scale was set at one times absorption, and the path-length was set at 40 meters.

C. TEMPERATURE MEASUREMENT AND CONTROL

During testing the canister was submerged in a water bath. The bath temperature was controlled by initially cooling with ice and then stabilizing the water bath temperature with a Neslab RTE-8 refrigerated circulating bath. The schematic of these is shown in Figure 1 and a photograph is shown in Figure 5.

Temperatures were monitored in the canister, at the exhaust of each flowmeter, and in the water bath with Omega stainless-steel-sheathed exposed-junction copper constantan thermocouples. The thermocouple outputs were directed through a 24-element switch to a Newport Model 267 digital pyrometer that indicated in degrees Fahrenheit. The thermocouples in the canister (shown in Figure 6) measured temperatures at the inside wall, one-inch radially from the wall and at two-inches radially (center of the canister axis) from the wall. The temperatures at these depths were monitored as the gas entered the Sodasorb, and at 1.75, 1.5, 1.5, 1.5, and 2.0-inch intervals thereafter along the length of the canister.

D. DESCRIPTION OF THE CANISTER

The canister (or container) for the Sodasorb was constructed from one-half-inch wall thickness four-inch inside

diameter acrylic plexiglas tubing of length twelve inches. Fine wire-mesh screens contained the Sodasorb at the gas entrance and exit. These square mesh screens were composed of .017 inches diameter wire of 18 squares per linear inch. The openings between the wires were .00149 square inches and 48% of the total cross sectional area was void between the wires.

Tail-piece spacers were utilized for changing the length of the canister bed of Sodasorb. Figures 7 and 8 illustrate the placement of these spacers.

The canister is further illustrated in Figures 9 and 10.

E. PRESSURE MEASUREMENTS WITHIN THE CANISTER

The axial pressure difference inside the canister of Sodasorb was monitored at points 1.75, 3.25, 4.75, 6.25, and 8.25 inches along the axis of the canister. Pressure-tap holes along the canister length were 1/16-inch diameter and connected to a manifold for selecting the desired pressure position. Pressures were indicated in inches of water on an Ellison four-inch inclined manometer, an Ellison 0.5-inch inclined manometer and a Flow Corporation micromanometer Model MM-2 connected in parallel.

IV. EXPERIMENTAL IDEALIZATIONS

Idealizations are required to model the flow of humid air and carbon dioxide mixtures through Sodasorb. The following assumptions were made:

1. Sodasorb is a homogenous porous media.
2. The flow is one-dimensional along the axis of the canister.
3. The gas obeys the perfect gas equation of state.
4. The gas flowing through the Sodasorb behaves as an incompressible fluid.

The procedures utilized to ensure that specific results would be consistent are listed in Appendix A.

V. PRESENTATION OF RESULTS

Figure 11 is the plot of the flow friction data in a form designed to enable the determination of the constants b and 1/k of equation 3b. The values of 1/k and b are determined from the least-squares linear relationship of these data points. Figure 12 displays the relationship of the Fanning friction factor for Sodasorb versus the Reynolds number utilizing $\sqrt{k}$ (0.004 inches) as the characteristic flow dimension. Included in Figure 12 for comparison purposes are the relationships of Darcy, Beavers and Sparrow, and Ward which are respectively 1/Re, 1/Re + 0.074 and 1/Re + 0.55. Table I lists the experimental results from which Figures 11 and 12 were formed.

Figure 13 illustrates the consistent infrared detector reading correlation to percentage of carbon dioxide in calibration gases.

Figures 14, 15 and 16 show the experimentally measured carbon dioxide exhausted from the canister as a function of time in nine representative experimental situations with 6.0% carbon dioxide by volume input.

In Figures 17, 18 and 19 the effectiveness of Sodasorb is plotted as a function of volumetric flow rate for 6.0% carbon dioxide input at constant length-to-diameter canister ratios of 1.225, 1.60 and 2.125 respectively. The results at temperatures of the incoming gas and canister environmental temperatures of 40°F, 55°F and 70°F are plotted.

The Sodasorb effectiveness dependence on length-to-diameter ratio for 6.0% carbon dioxide input at constant temperatures are shown in Figures 20, 21 and 22.

Figures 23, 24 and 25 plot the effectiveness of Sodasorb as a function of length-to-diameter ratio with a volumetric flow rate of approximately 2 SCFM.

The experimental data are recorded in Tables II, III and IV.

VI. DISCUSSION OF RESULTS

The characteristic flow dimension ($\sqrt{k}$) obtained from Figure 11 was obtained by the same method used by Ward in 1964 and Beavers and Sparrow in 1969. Ward passed water through approximately spherical glass beads, sand, gravel, anthracite coal and granular activated carbon with some media being uniform in size and others varying widely in size distribution. Ward showed a smooth transition in porous media from what he defines as laminar to turbulent flow. Beavers and Sparrow passed water through non-granular fibrous lattice materials and defined the departure from laminar flow as being due to inertia effects (first separation, wake effects and form drag) then later as turbulence. These experiments, using differing materials as a porous media, demonstrated that straight lines were the only satisfactory representation of data when plotted as in Figure 11. Beavers and Sparrow utilized velocities spanning a range of 20-to-1 and experienced a scatter of only 2.5% from the least-squares relationship. Ward utilized a range of velocity that was not as inclusive and his data had considerably more scatter in the plotted points. Beavers and Sparrow determined that a good value for c in their non-granular media was 0.074 while Ward proposed 0.55 for his granular media. As can be seen in Figure 12 the value experimentally determined for Sodasorb using a gas as the fluid fits extremely well with the data determined by Ward. The maximum scatter for Sodasorb in

Figure 11 was 8.2%. (This maximum value was an end-point in the humid air testing which was obtained with a pressure drop slightly greater than 0.5 inches of water. It was the only data point that had to be read on the 4-inch rather than the 0.5-inch inclined manometer). The differences in the results of Beavers and Sparrow and the results from this experiment may be attributed to the type and texture of the porous media being tested.

The Fanning friction factor for Sodasorb porous media, as seen in Figure 12 and Table I, can properly be represented by $f = 1/Re + 0.55$.

The resistance to flow as defined by Elam [10] results in values of the axial pressure drop in Sodasorb of approximately twice those experimentally determined herein.

Figures 14, 15 and 16 demonstrate the negligible amount of carbon dioxide that exits the canister prior to reaching 0.5% by volume in the exhaust gas. These plots clearly illustrate the similarity of all representative runs in these non-dimensional curves.

As predicted prior to experimentation, the flow rate of the gas passing through a bed of Sodasorb is an important parameter in the effectiveness of Sodasorb to remove carbon dioxide. As discerned in Figures 17 through 22 the effectiveness consistently increases in a nonlinear way as the volumetric flow rate decreases.

As the inlet gas and environmental temperature increase, the effectiveness of Sodasorb increases in the ranges tested

as shown in Figures 17 through 25. It is also evident in Figures 17 through 25 that the shorter length-to-diameter ratios with the least effectiveness are less sensitive to temperature changes in the ranges tested.

A qualitative assessment of indications occurring during this experimentation may assist future exploration in defining the variables in the effectiveness of Sodasorb to remove carbon dioxide from a gas. The acid-base color indicator in Sodasorb reacted differently for various flow rates and percentage inputs of carbon dioxide.

At the slower flow rates and lower carbon dioxide input proportions, the dark blue color change moved very slowly along the length of the canister. The rate of progression of the front along the wall appeared to be constant. Using this and an observed initial rate, the time for the front to reach the end of the canister, and hence the termination of the run was fairly well predictable. As the flow rate and/or the proportion of carbon dioxide was increased the light blue color change moved more rapidly along the wall of the canister. An estimation of the rapid time to termination based upon the color change was inconsistent when compared with the measured true time to termination.

Upon completion of most experimental runs an attempt was made to visually inspect the inner contents of the canister for color change. Difficulties in rapid disassembly of the close fitting, sometimes warm, components of the canister were encountered. The general indication upon disassembly

was dark central color changes from slower flow rates and lower carbon dioxide input percentages; and lighter color changes with higher flow rates and higher carbon dioxide input percentages. The color limits were as described by the manufacturer of Sodasorb, that is, a parabolic shaped darker section with the apex of the parabola being nearest the exhaust end of the canister. No color indication, however, was witnessed that would indicate utilization of the Sodasorb along the walls in preferential paths.

After dumping the contents of the canister into an open pail exposed to ambient atmosphere the color would usually change rapidly to white. When the slower flow rates and lower carbon dioxide percentages had turned the color of the Sodasorb to dark blue the color was observed to remain in the Sodasorb in the pail in excess of 24 hours.

VII. CONCLUSIONS

The following conclusions may be made from the results of this investigation:

1. The characteristic flow dimension for Sodasorb was experimentally determined to be 0.004 inches.
2. The Fanning friction factor for Sodasorb can be represented as:

$$f = \frac{1}{Re} + 0.55$$

3. The effectiveness of Sodasorb to remove carbon dioxide from a gas was experimentally determined to be inversely related to the flow rate in the ranges tested.
4. The temperatures of the incoming gas and canister environment as well as the length-to-diameter ratio were experimentally determined to have a significant effect on the effectiveness of Sodasorb to remove carbon dioxide from a gas.

VIII. RECOMMENDATIONS FOR FURTHER STUDY

The results of this initial experimentation with steady flow rates through Sodasorb posed questions that may merit further examination:

1. It may improve the effectiveness of Sodasorb if baffles, screens, or flow deflectors are added to the canister, as has been demonstrated in anesthesiology.
2. Effects of actual diving systems, such as damping of the diver's breathing signature, should be examined to determine the type of flow actually experienced in the canisters of such systems.
3. A study of the relationships between steady flow and unsteady flow is necessary to correlate these results with those of canisters in actual breathing systems.
4. Canister length-to-diameter ratios of approximately one-to-six are being considered for newer diving systems and require analysis.
5. The effectiveness in these experiments was based upon the canister being used in a stationary horizontal mode. Further testing is necessary to determine dependence upon movement and orientation.
6. The effect of increased pressure on the effectiveness of Sodasorb is presently unknown.
7. The effectiveness differences between batches or possibly even containers of Sodasorb should be

determined prior-to or during further examination of canister geometry.

8. Real-time continuous recording of inside canister temperatures is necessary to quantitatively correlate effectiveness results to reaction temperatures.

TABLE I. FLOW FRICTION RESULTS FOR SODASORB

	NITROGEN				AIR FROM BANKS				HUMID AIR				DIMENSIONS
T_3	70	68	64	63	63	63	62	62	64	69	72	72	^oF
T_4	69	69	65	64	63	63	63	62	64	68	71	72	^oF
T_9	68	55	50	49	56	55	54	53	66	76	74	71	^oF
T_{10}	68	62	51	50	54	56	54	54	58	75	74	71	^oF
T_{15}	66	52	47	48	53	53	52	52	68	77	74	70	^oF
T_{16}	67	58	48	48	50	54	52	52	56	77	74	70	^oF
T_{20}	71	71	67	64	69	70	70	70	72	72	71	71	^oF
$\bar{T}_c$	68.0	61.1	54.3	53.7	56.4	57.4	56.2	55.9	62.1	73.6	73.1	71.0	^oF
ΔP_L	.0615	.185	.337	.4595	.063	.1925	.3425	.476	.128	.2365	.3805	.509	in. H_2O
Q_f	.69	1.61	2.553	3.243	.69	1.61	2.53	3.22	1.15	1.84	2.53	3.22	ft^3/min
P_f	14.653	14.689	14.761	14.826	14.649	14.696	14.758	14.826	15.195	15.487	15.884	16.300	lb/in^2
μ_c	42.5	42.0	41.5	41.5	43.0	43.2	43.0	43.0	43.5	44.3	44.1	44.0	$lbm/ft\text{-}hr \times 10^{-3}$
μ_f	42.5	42.5	42.5	42.2	44.0	44.0	44.0	44.0	44.0	44.0	44.0	44.0	$lbm/ft\text{-}hr \times 10^{-3}$
R	55.15	55.15	55.15	55.15	53.34	53.34	53.34	53.34	53.34	53.34	53.34	53.34	$ft\text{-}lb/lbm\text{-}^oR$
$P_{atm}=$	$P_c = 14.635$ lb/in^2												
$\frac{\rho_c V_c}{\mu_c}$	804.3	1903.7	3093.4	3969.3	824.8	1918.1	3041.0	3888.2	1401.6	2244.3	3185.4	4169.7	1/ft
$\frac{-\frac{dp}{dx}}{\mu_c V_c}$	9.66	12.74	14.82	15.77	9.97	12.95	14.71	15.99	11.52	12.54	14.36	14.80	$1/ft^2 \times 10^6$
$\bar{k}$	111.3		117.0				114.5				101.5		$ft^2 \times 10^{-9}$
$\sqrt{k}$	333.6		342.0				338.4				318.6		$ft \times 10^{-6}$
b	1708.1		1924.0				1932.5				1255.0		1/ft
c	569.8		658.0				654.0				399.8		N.D. $\times 10^{-3}$
Re	.2683	.6350	1.0319	1.3241	.2751	.6399	1.0144	1.2971	.4675	.7487	1.0626	1.3910	N.D.
f	4.0081	2.2329	1.5987	1.3254	4.0320	2.2525	1.6131	1.3721	2.7419	1.8639	1.5036	1.1838	N.D.
f'	4.2969	2.1445	1.5389	1.3250	4.2043	2.1326	1.5556	1.3408	2.7086	1.9055	1.5109	1.2887	N.D.

TABLE II

SODASORB EFFECTIVENESS RESULTS FOR L/D = 1.60

Run #	L/D	T (^{o}F)	Q_s (SCFM)	CO_2% Input	$t_{1/2}$ (min)
1	1.60	70	2.07	4.0	42.5
2	1.60	70	2.29	6.0	21
3	1.60	70	2.14	8.0	12
4	1.60	70	1.06	6.0	66
5	1.60	70	3.30	6.0	4
6	1.60	55	2.17	4.0	18
7	1.60	55	2.20	6.0	8
8	1.60	55	2.24	8.0	6
9	1.60	55	1.10	6.0	45
10	1.60	55	3.24	6.0	6
11	1.60	40	2.24	4.0	12
12	1.60	40	2.20	6.0	13
13	1.60	40	2.32	8.0	13
14	1.60	40	1.20	6.0	28
15	1.60	40	3.52	6.0	5

TABLE III

SODASORB EFFECTIVENESS RESULTS FOR L/D = 2.125

Run #	L/D	T (^{o}F)	Q_s (SCFM)	CO_2% Input	$t_{1/2}$ (min)
16	2.125	70	2.16	4.0	58.5
17	2.125	70	2.23	6.0	28
18	2.125	70	2.21	8.0	24
19	2.125	70	1.07	6.0	78
20	2.125	70	3.39	6.0	9
21	2.125	55	2.18	4.0	39
22	2.125	55	2.12	6.0	22.5
23	2.125	55	2.11	8.0	19
24	2.125	55	1.08	6.0	46.5
25	2.125	55	3.27	6.0	10.5
26	2.125	40	2.13	4.0	26
27	2.125	40	2.20	6.0	16.5
28	2.125	40	2.09	8.0	18
29	2.125	40	1.10	6.0	63.5
30	2.125	40	3.30	6.0	9

TABLE IV

SODASORB EFFECTIVENESS RESULTS FOR L/D = 1.225

Run #	L/D	T (^{o}F)	Q_s (SCFM)	CO_2% Input	$t_{1/2}$ (min)
31	1.225	70	2.18	4.0	9
32	1.225	70	2.19	6.0	9
33	1.225	70	2.23	8.0	10
34	1.225	70	1.14	6.0	27
35	1.225	70	3.78	6.0	2.5
36	1.225	55	2.24	4.0	10
37	1.225	55	2.19	6.0	5.5
38	1.225	55	2.32	8.0	8
39	1.225	55	1.10	6.0	30.5
40	1.225	55	3.64	6.0	4
41	1.225	40	2.36	4.0	11
42	1.225	40	2.23	6.0	7
43	1.225	40	2.28	8.0	7
44	1.225	40	1.13	6.0	29
45	1.225	40	3.63	6.0	4

FIGURE 1. EQUIPMENT SCHEMATIC

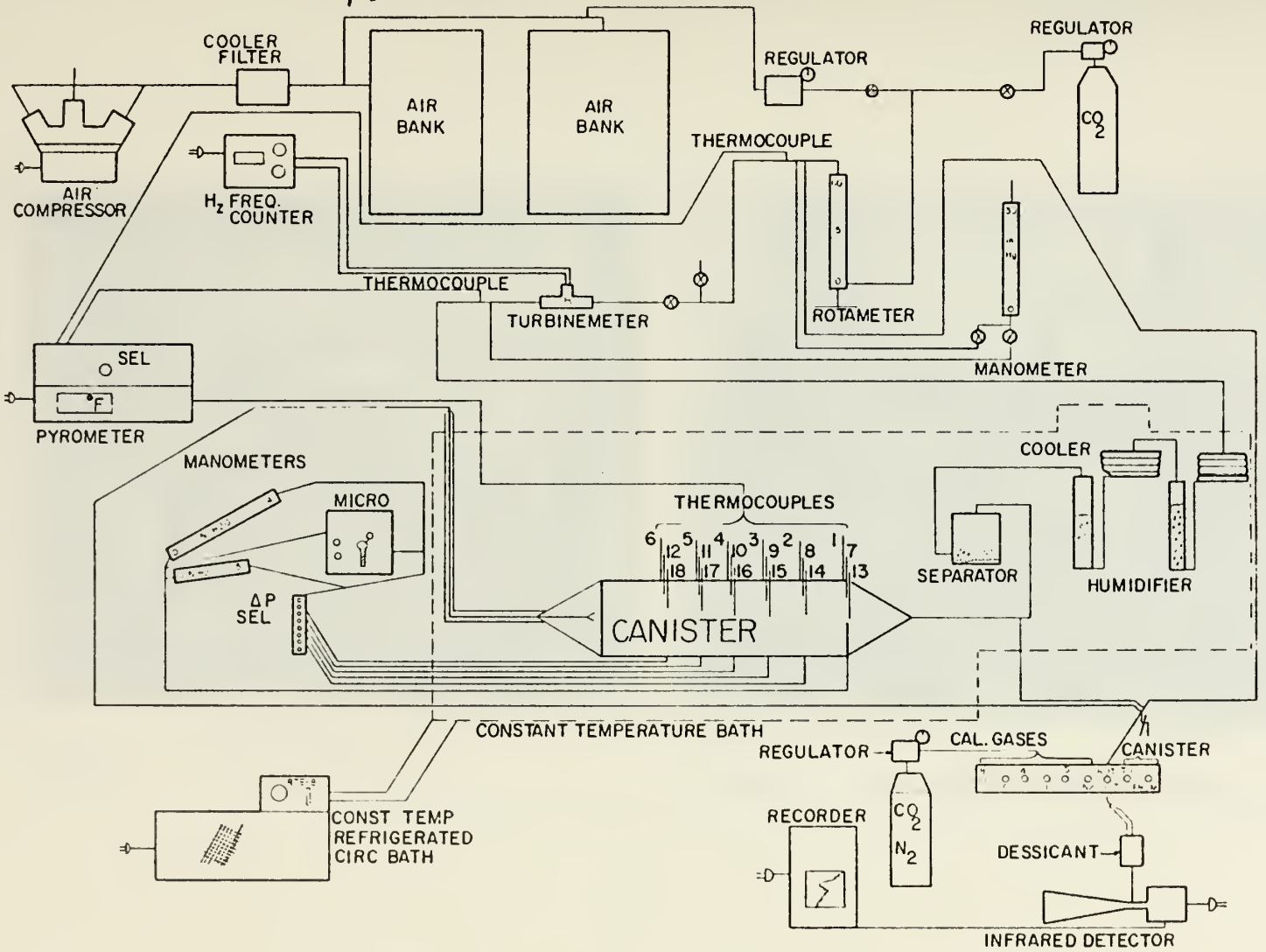

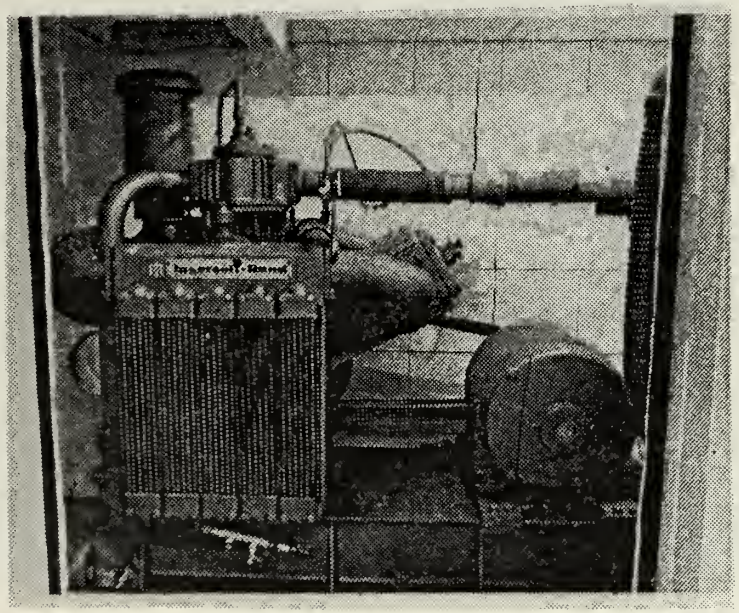

FIGURE 2. Air Compressor.

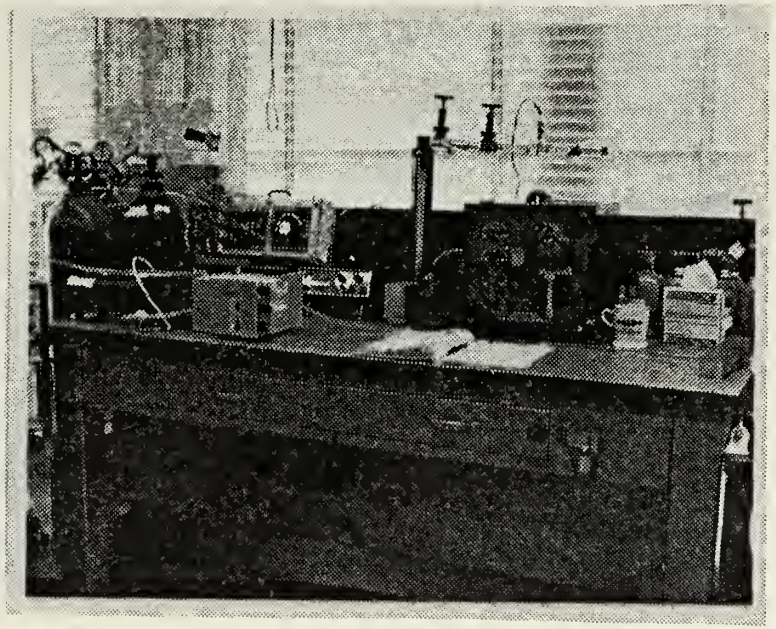

FIGURE 3. Flowmeters and Infrared Detector

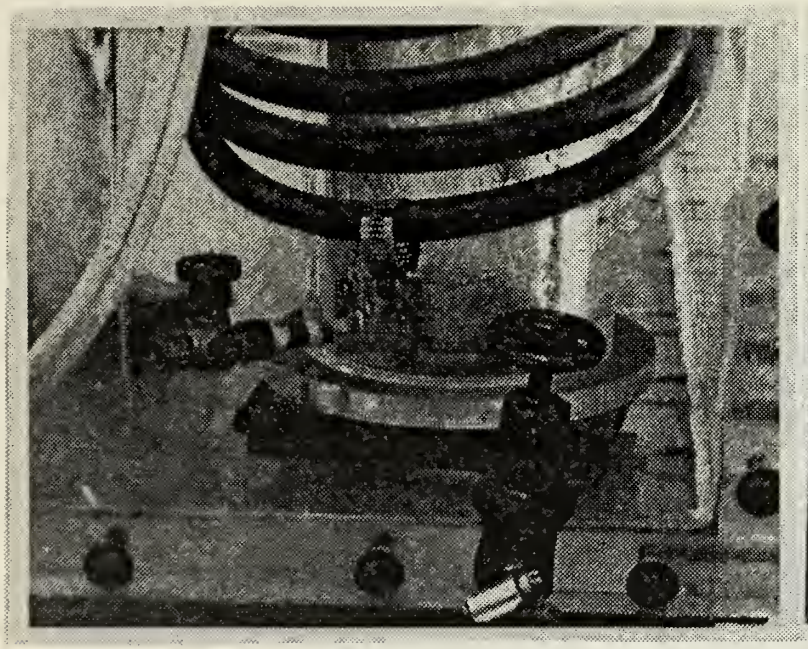

FIGURE 4. Primary Water Separator

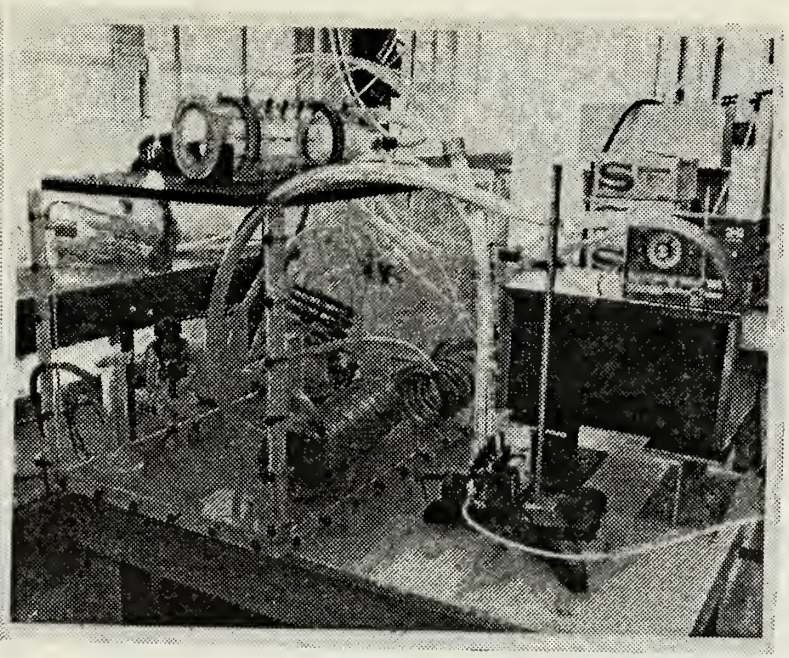

FIGURE 5. Constant Temperature Bath

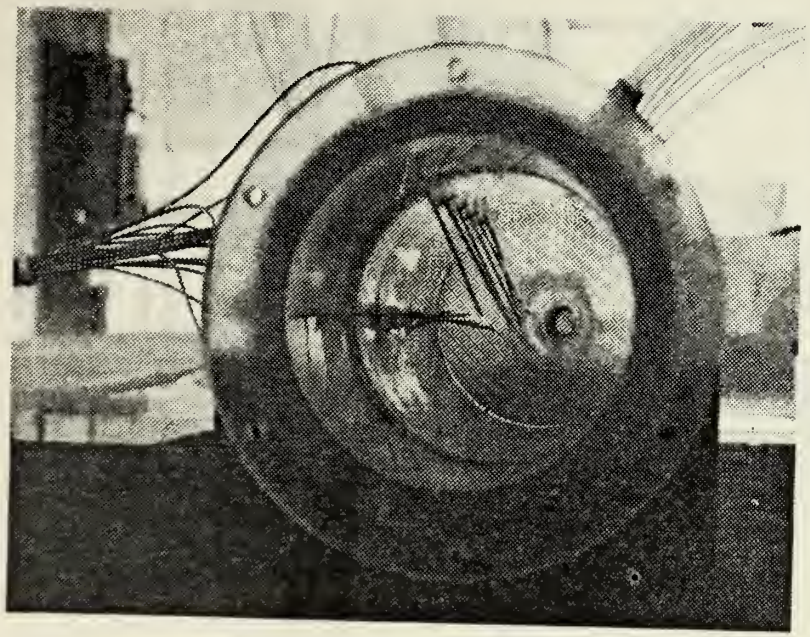

FIGURE 6. Canister (Internal)

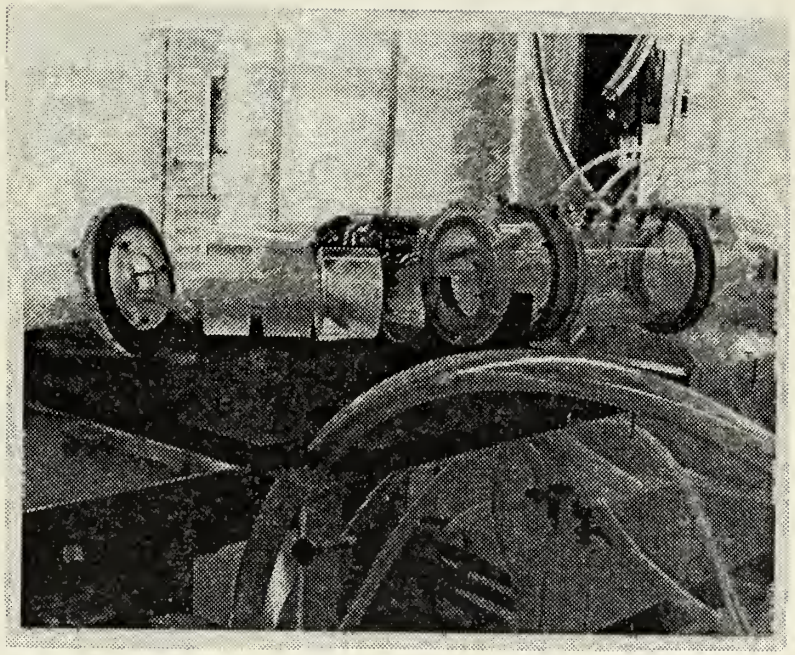

FIGURE 7. Canister Assembly

FIGURE 8. Canister

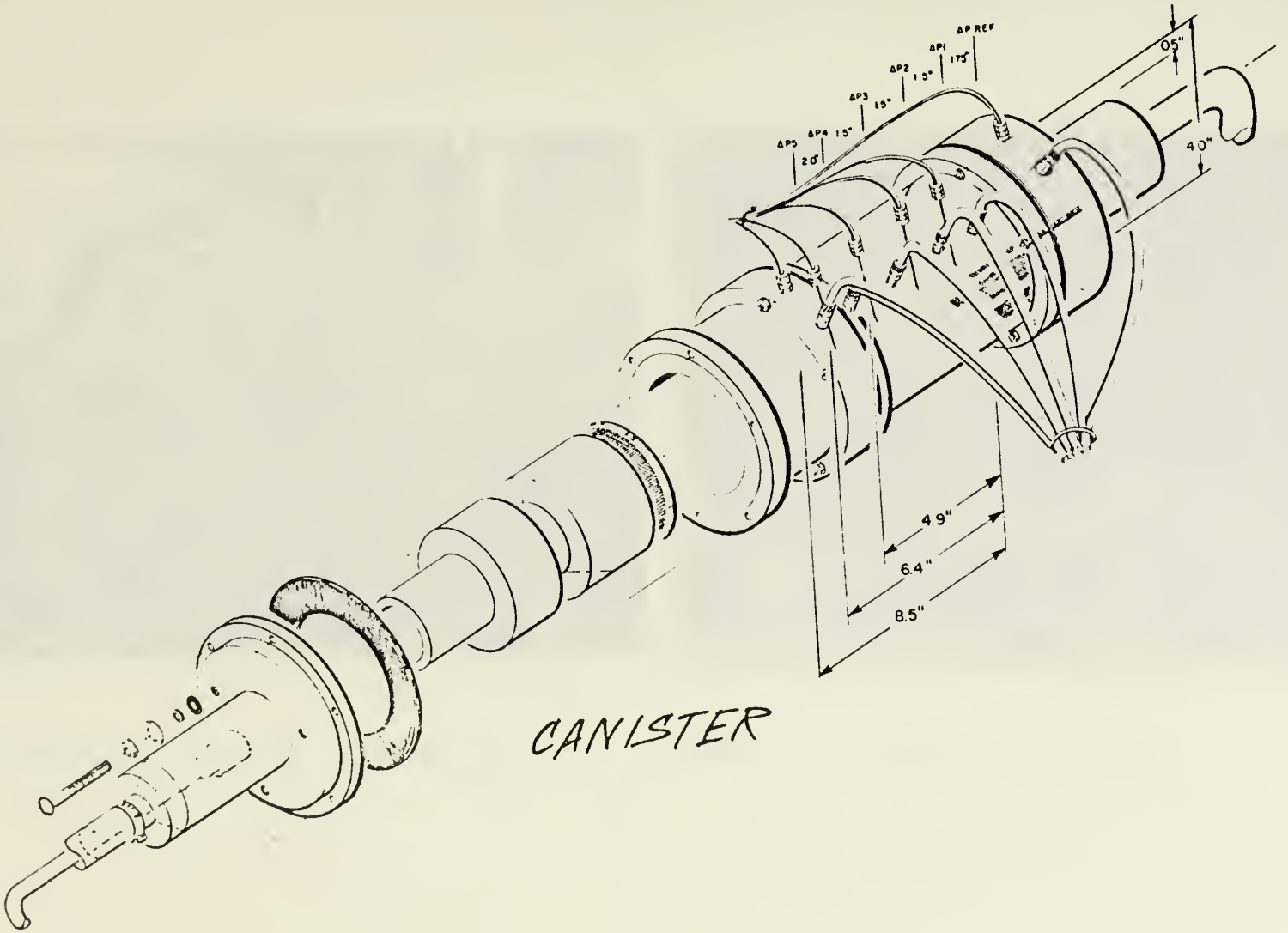

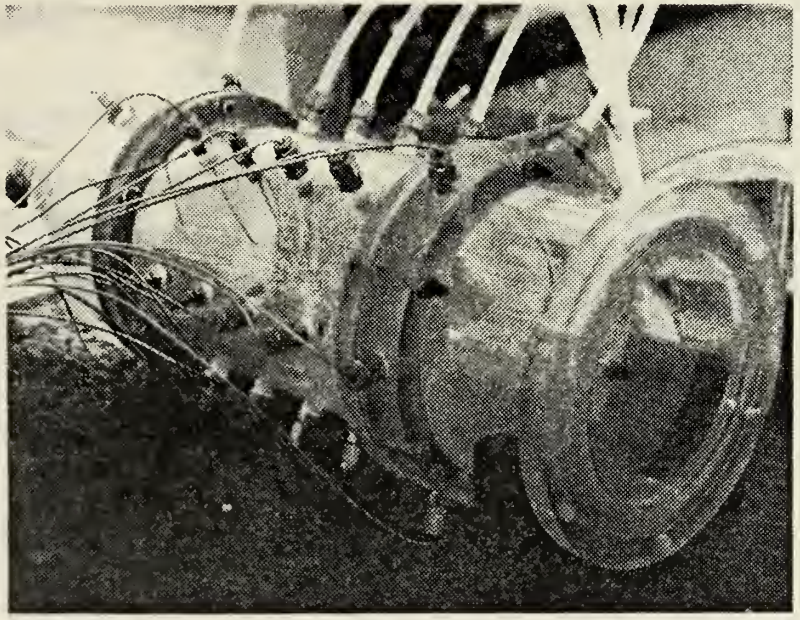

FIGURE 9. Canister (External)

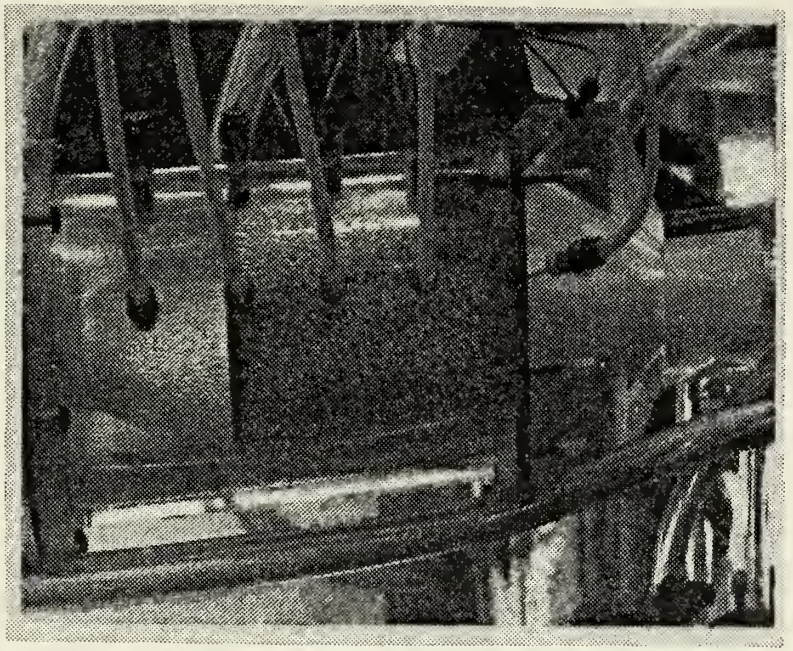

FIGURE 10. Canister (In Use)

FIGURE 11.

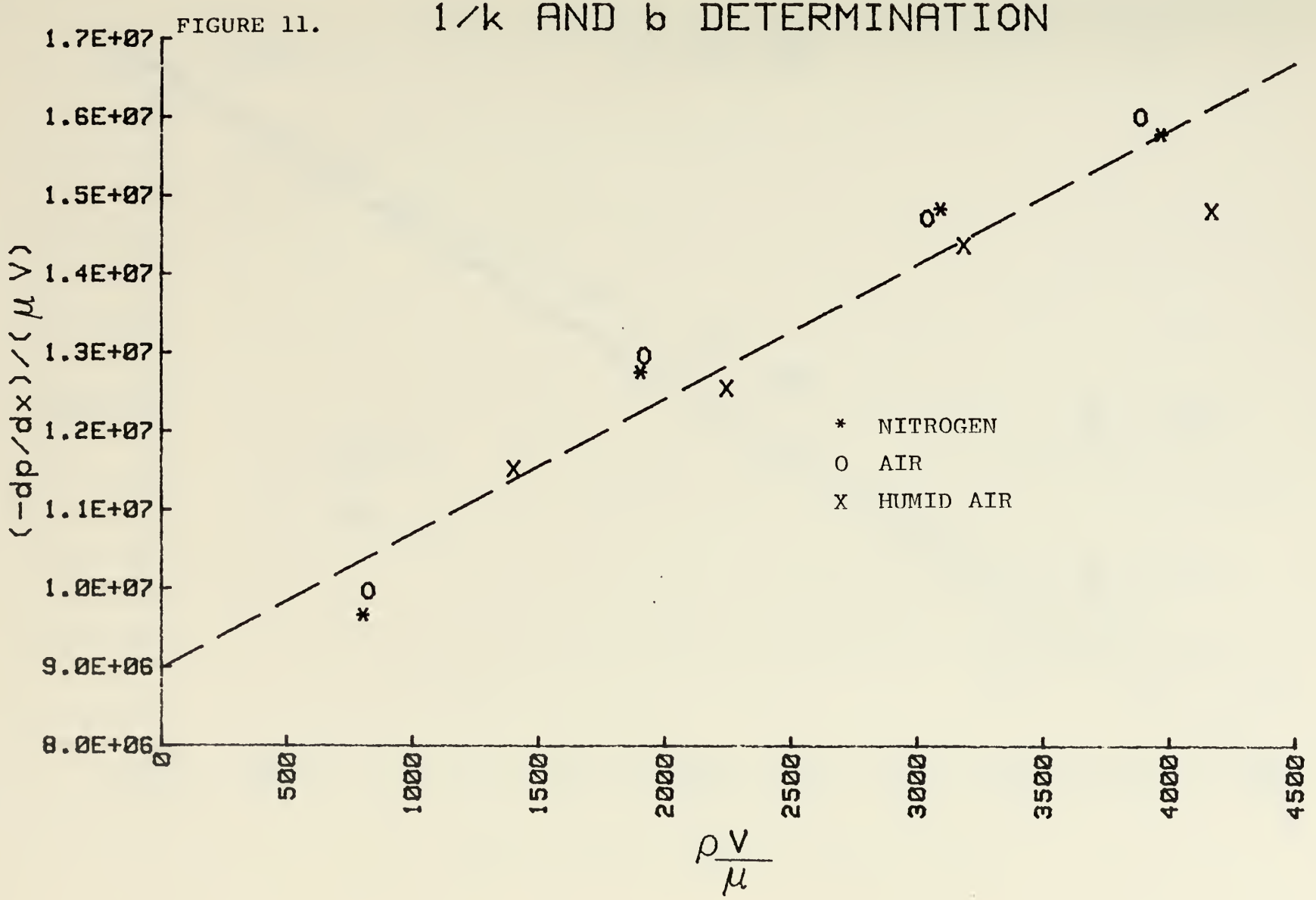
1/k AND b DETERMINATION
1.7E+07
1.6E+07
1.5E+07
1.4E+07
1.3E+07
1.2E+07
1.1E+07
1.0E+07
9.0E+06
8.0E+06
(-dp/dx)/(μV)
0
500
1000
1500
2000
2500
3000
3500
4000
4500
ρV/μ
* NITROGEN
O AIR
X HUMID AIR

FIGURE 12.

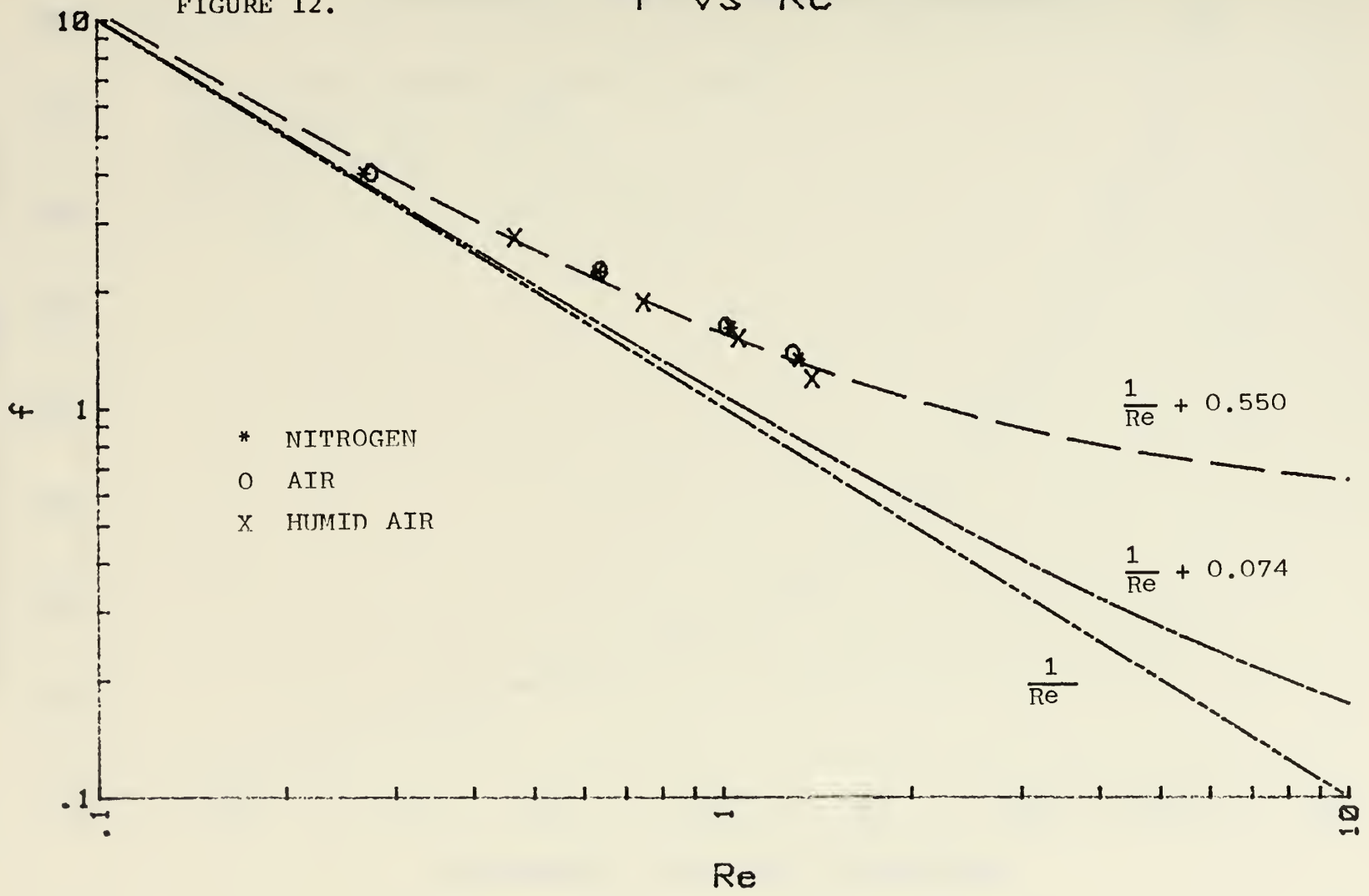
f vs Re
10
1
.1
f
1
10
Re
* NITROGEN
O AIR
X HUMID AIR
1/Re + 0.550
1/Re + 0.074
1/Re

FIGURE 13. INFRARED CO2 RELATIONSHIP

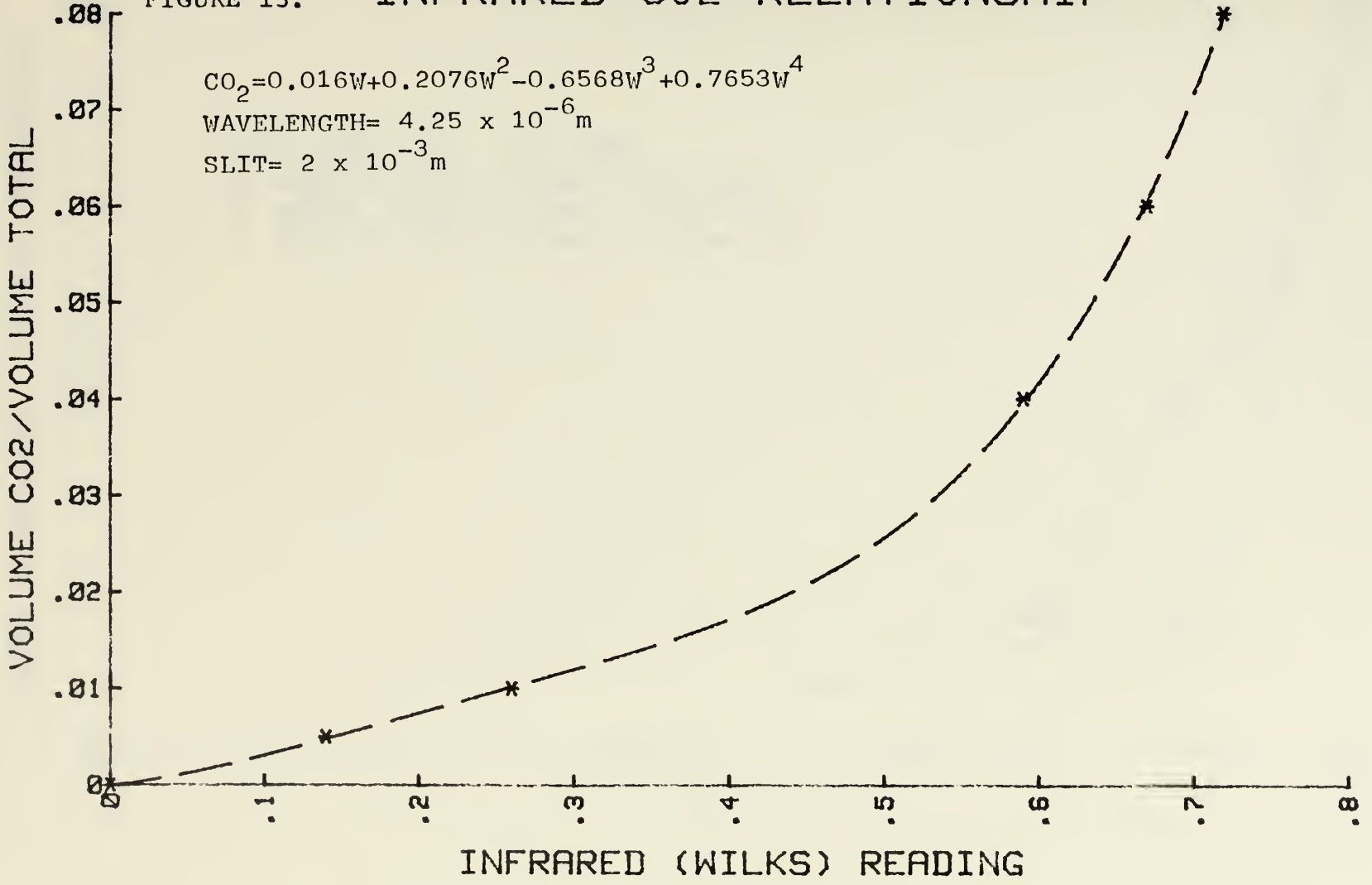

FIGURE 14.

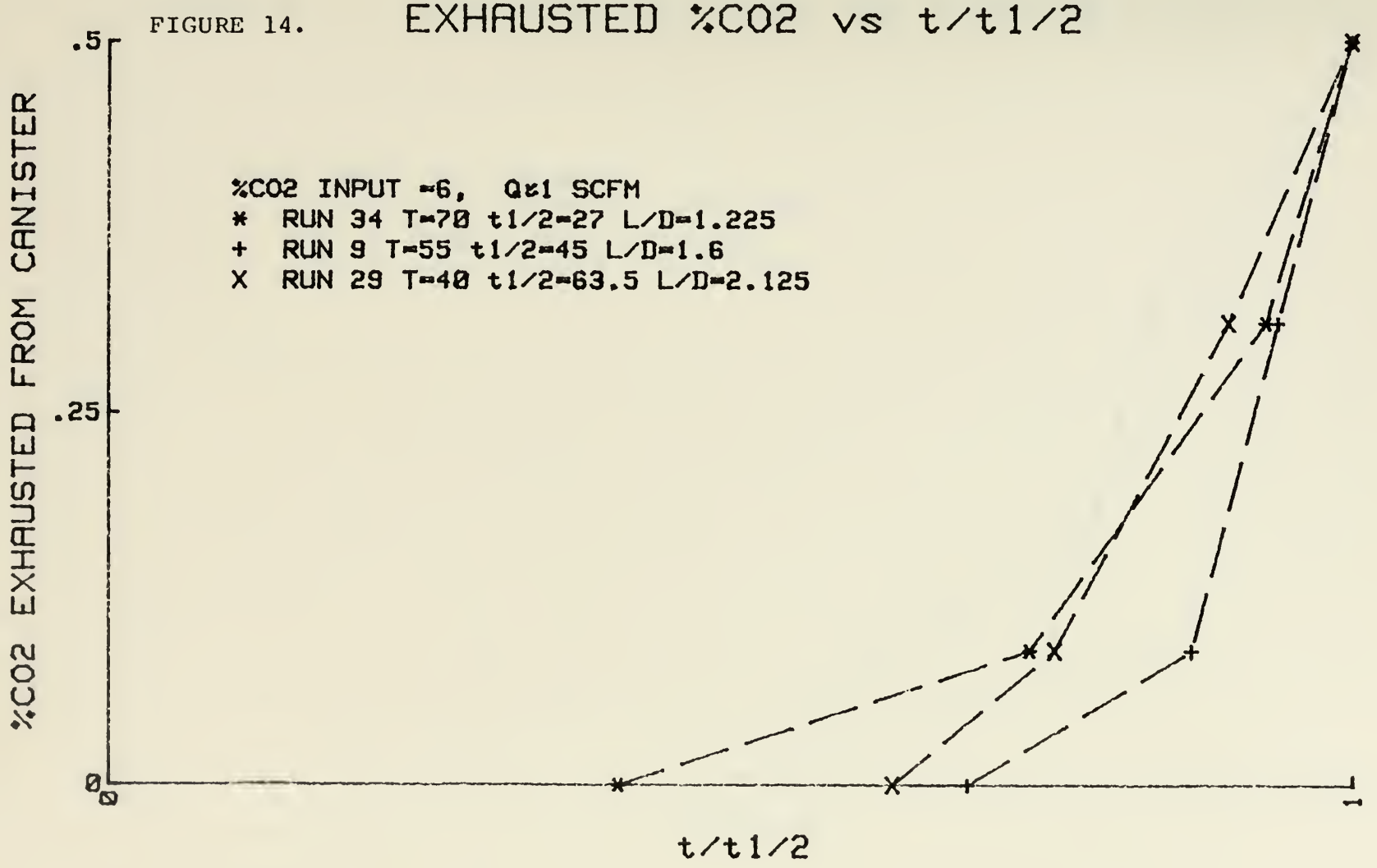
EXHAUSTED %CO2 vs t/t1/2
%CO2 INPUT =6, Q≈1 SCFM
* RUN 34 T=70 t1/2=27 L/D=1.225
+ RUN 9 T=55 t1/2=45 L/D=1.6
X RUN 29 T=40 t1/2=63.5 L/D=2.125
%CO2 EXHAUSTED FROM CANISTER
.5
.25
0
0
1
t/t1/2

FIGURE 15.

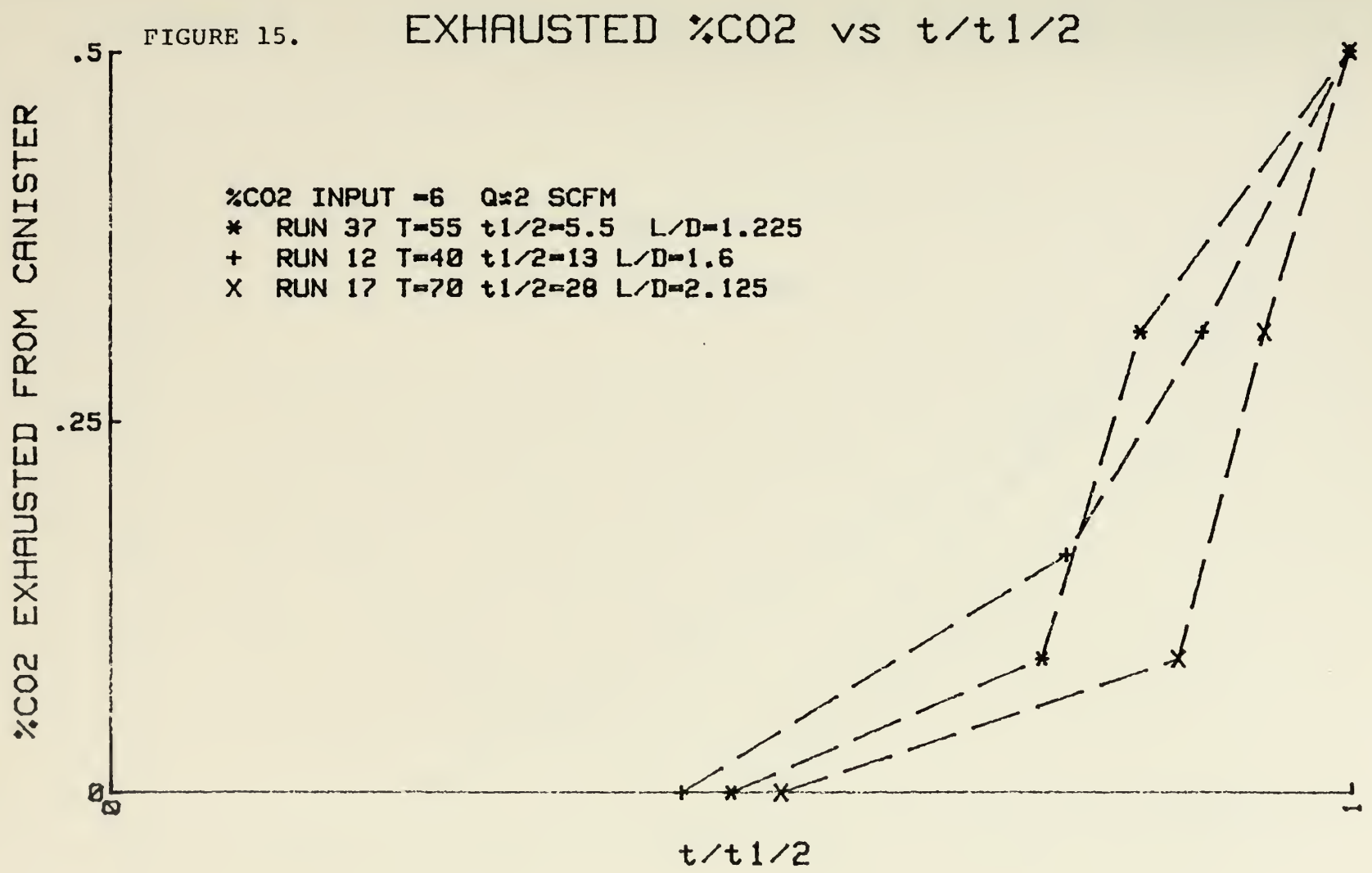
EXHAUSTED %CO2 vs t/t1/2
%CO2 INPUT =6 Q=2 SCFM
* RUN 37 T=55 t1/2=5.5 L/D=1.225
+ RUN 12 T=40 t1/2=13 L/D=1.6
X RUN 17 T=70 t1/2=28 L/D=2.125
%CO2 EXHAUSTED FROM CANISTER
.5
.25
0
0
1
t/t1/2

FIGURE 16.

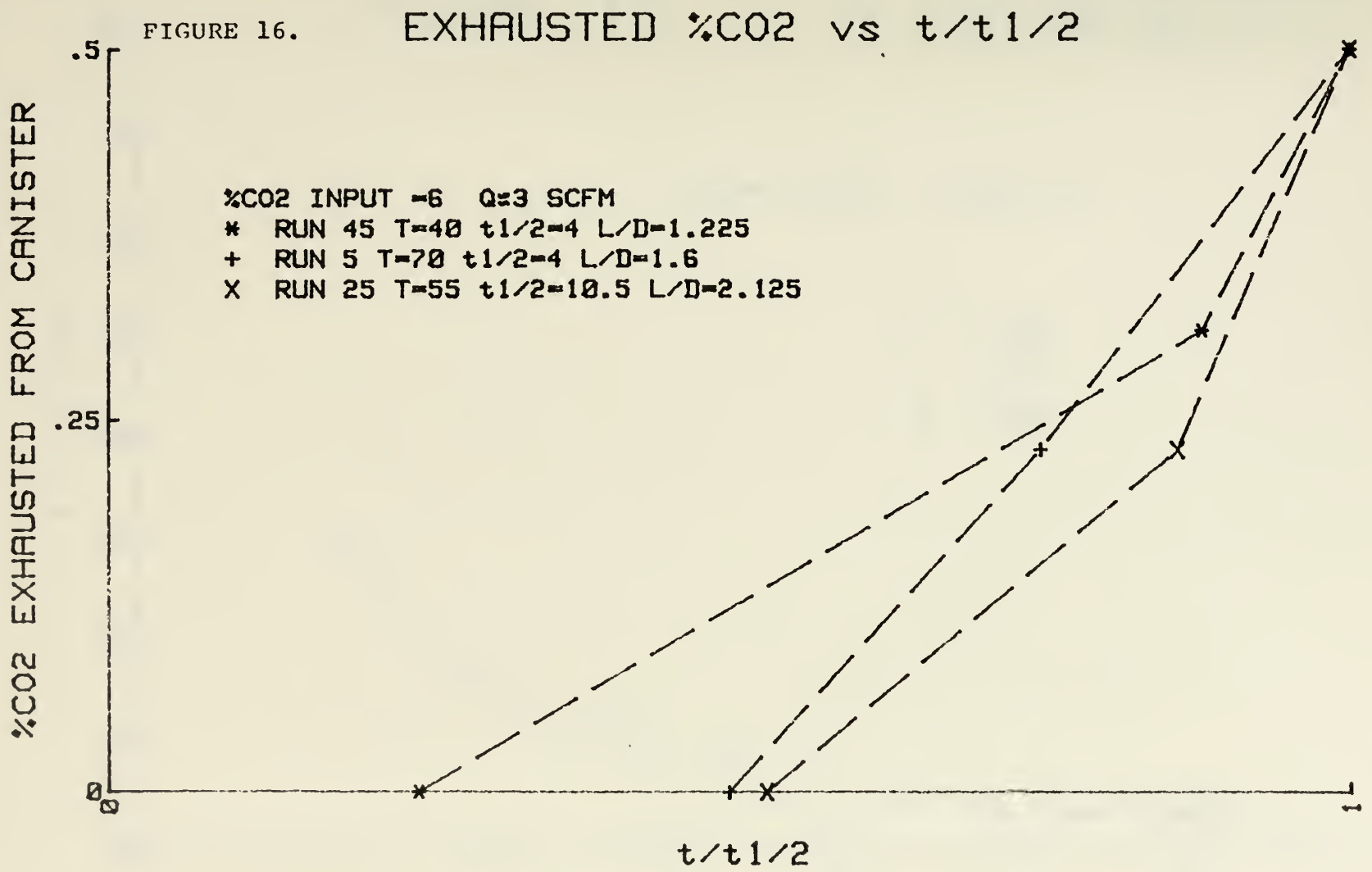
EXHAUSTED %CO2 vs t/t1/2
%CO2 EXHAUSTED FROM CANISTER
.5
.25
0
0
1
t/t1/2
%CO2 INPUT =6 Q=3 SCFM
* RUN 45 T=40 t1/2=4 L/D=1.225
+ RUN 5 T=70 t1/2=4 L/D=1.6
X RUN 25 T=55 t1/2=10.5 L/D=2.125

FIGURE 17 t 1/2 vs Q

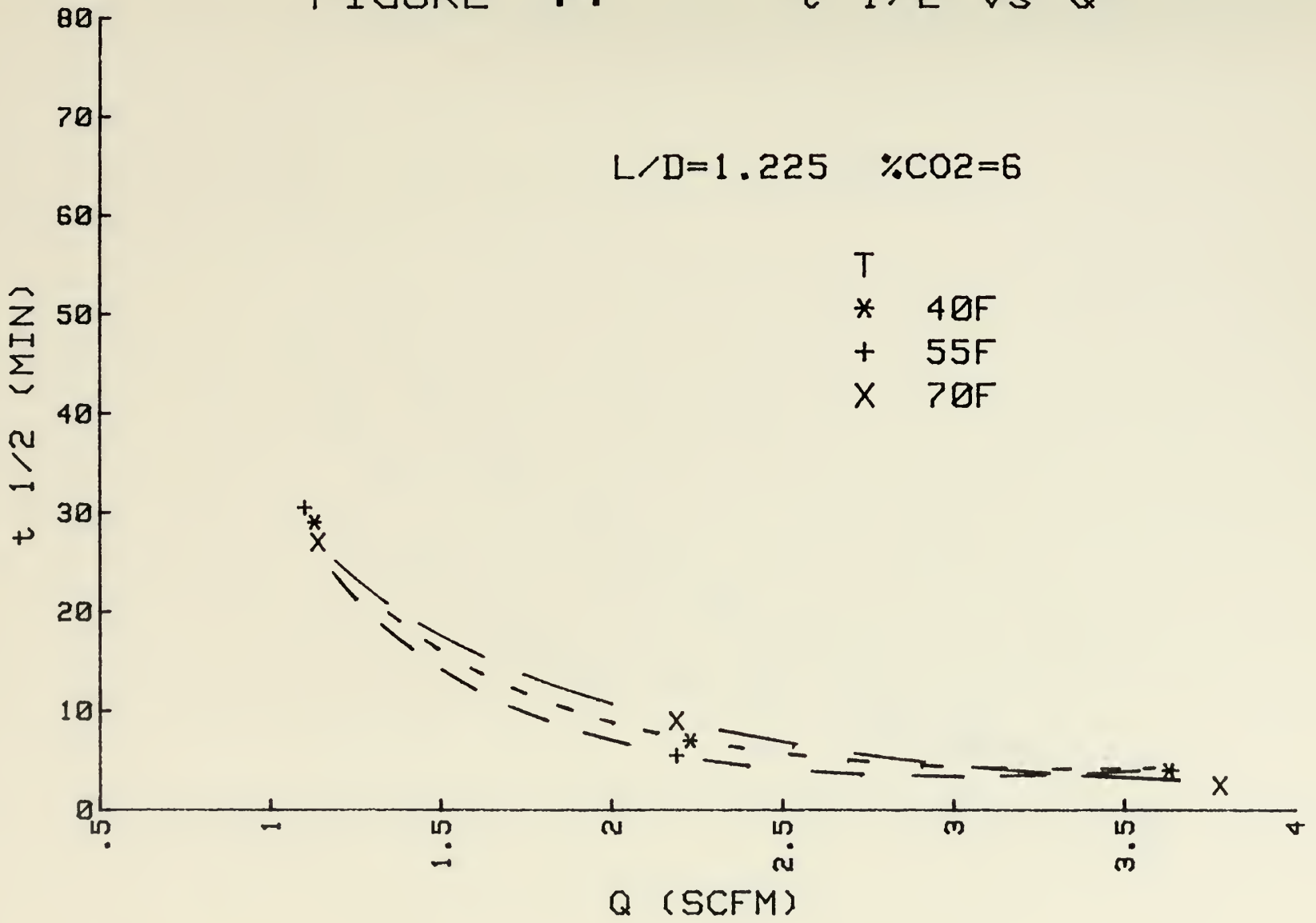

FIGURE 18 t 1/2 vs Q

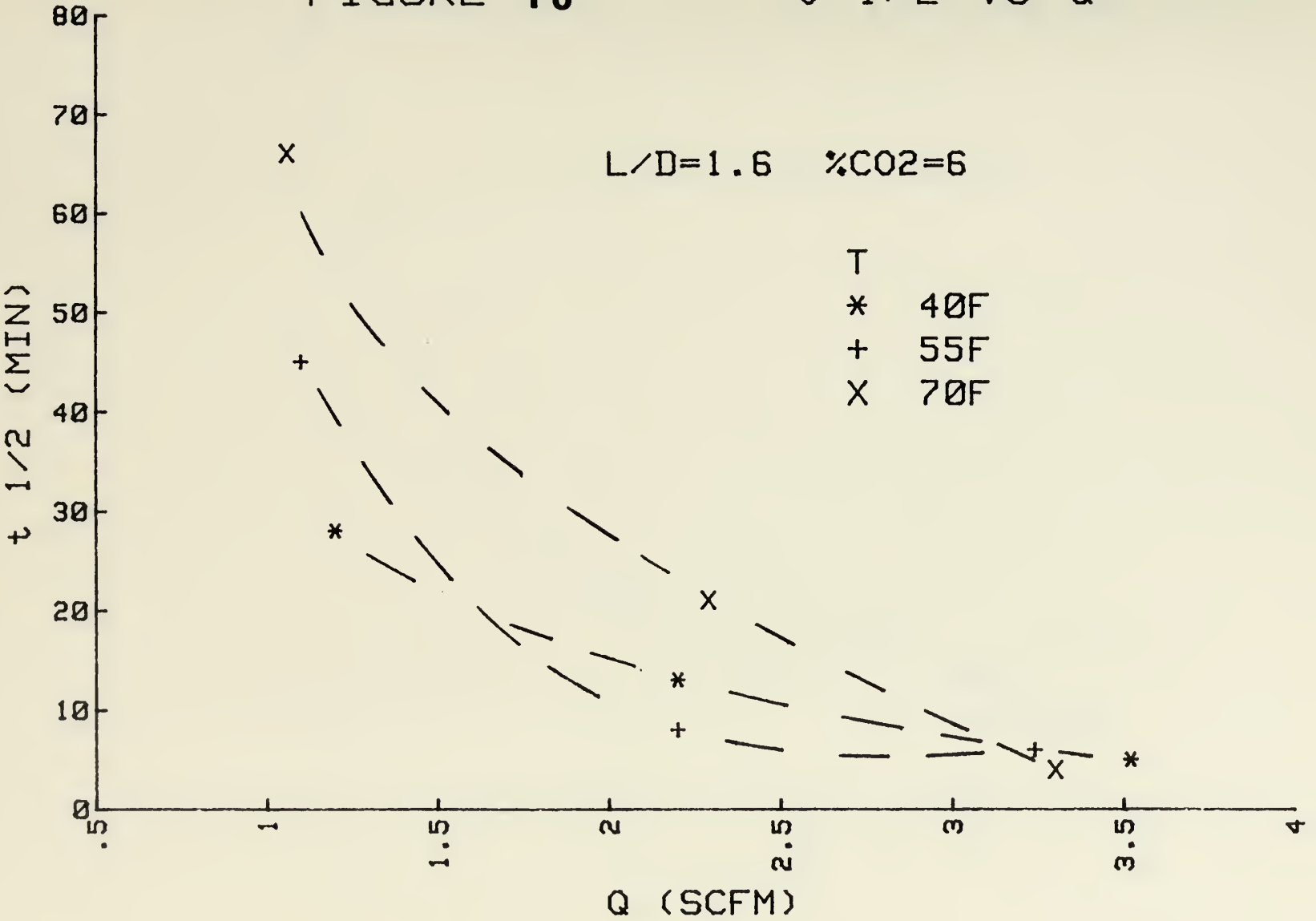

FIGURE 19 t 1/2 vs Q

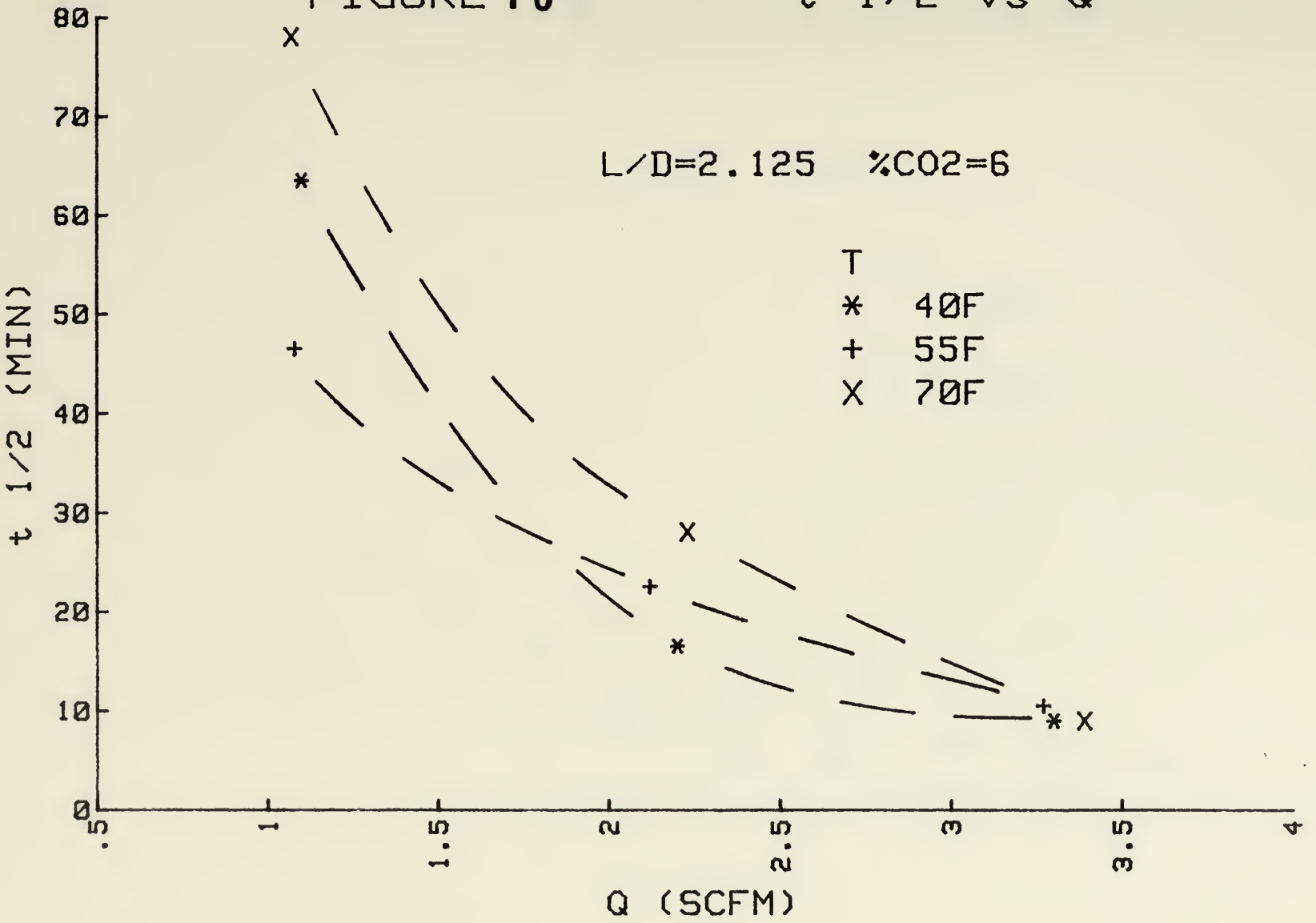

FIGURE 20 t 1/2 vs Q

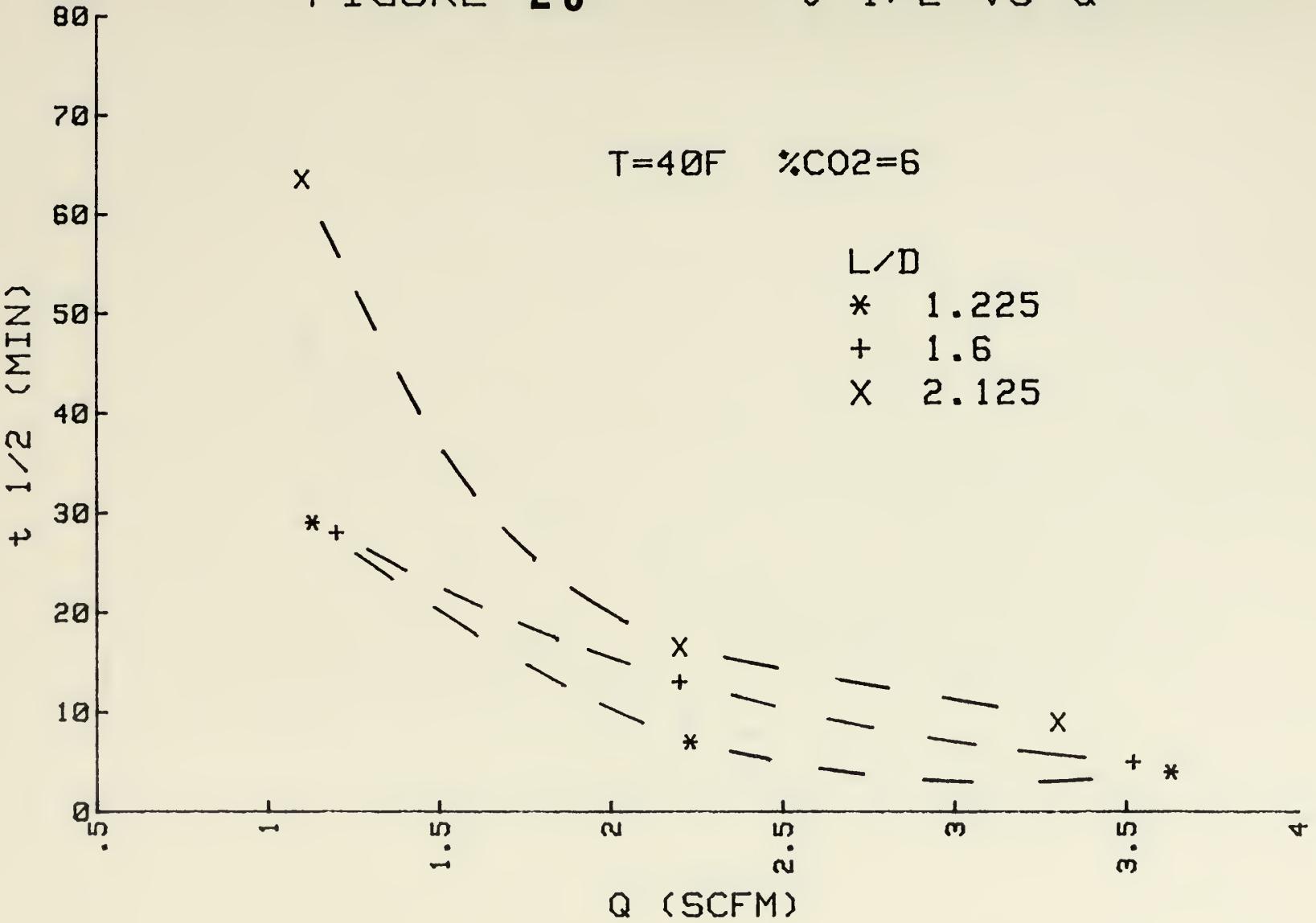

FIGURE 21 t 1/2 vs Q

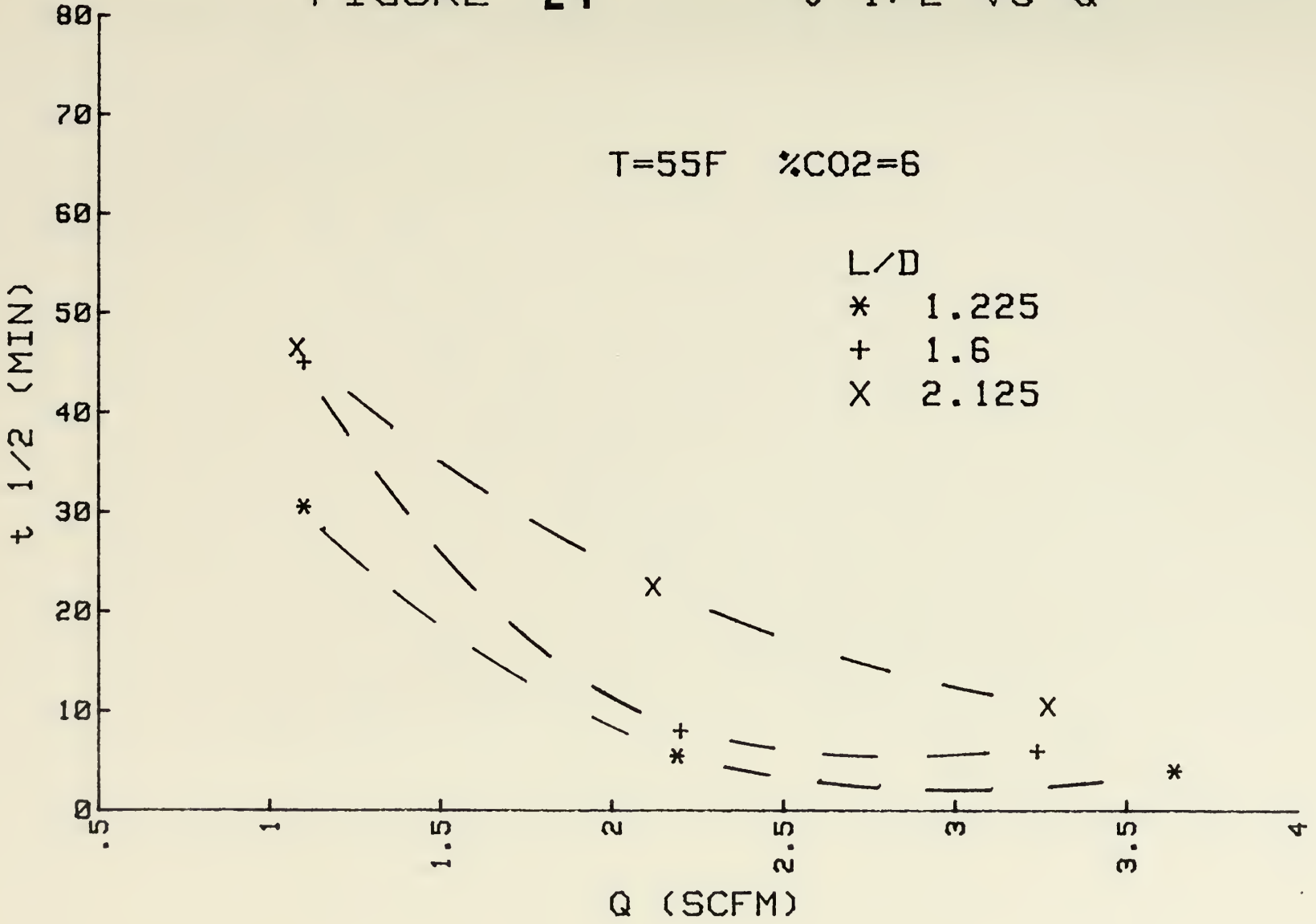

FIGURE 22 t 1/2 vs Q

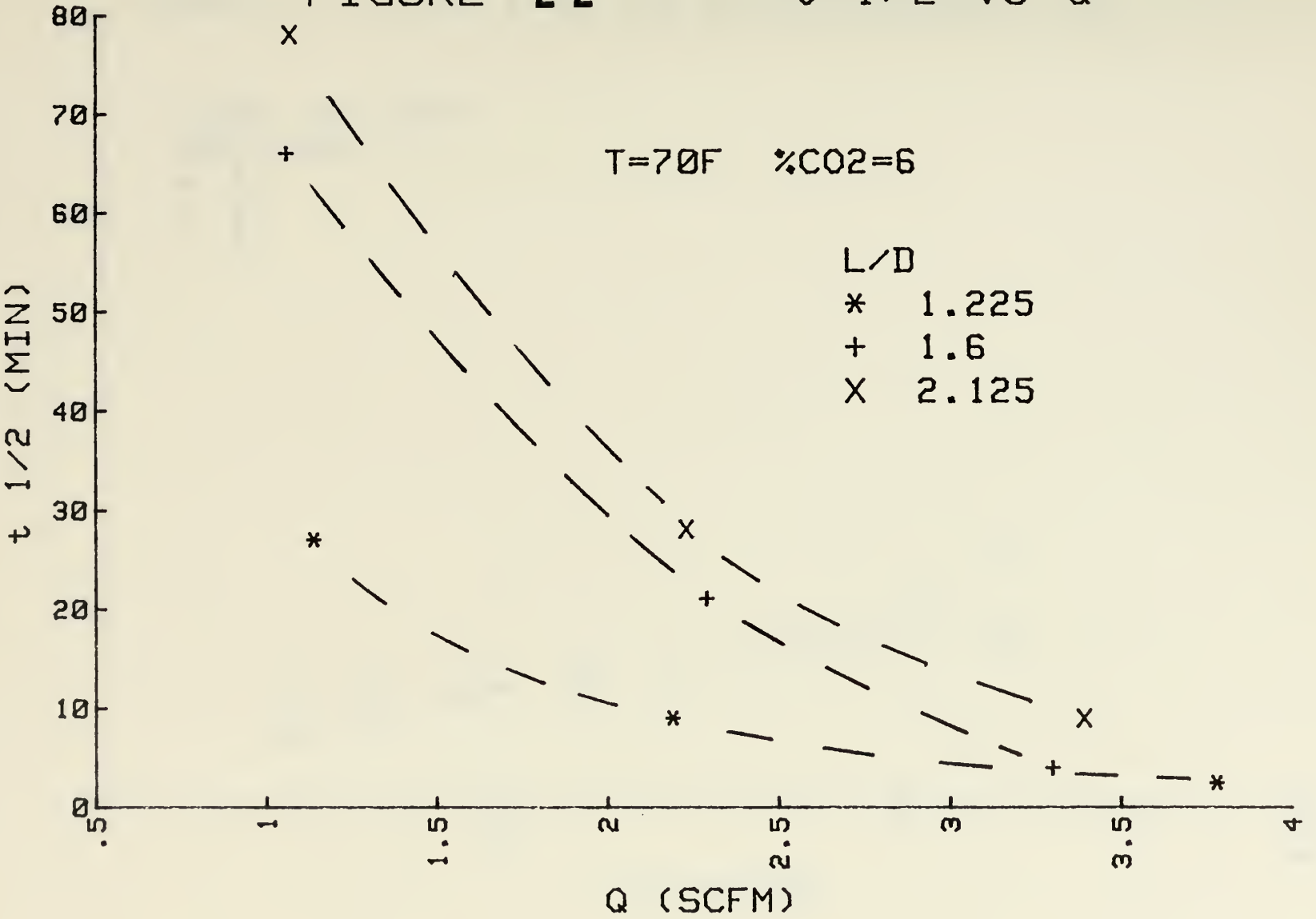

FIGURE 23.

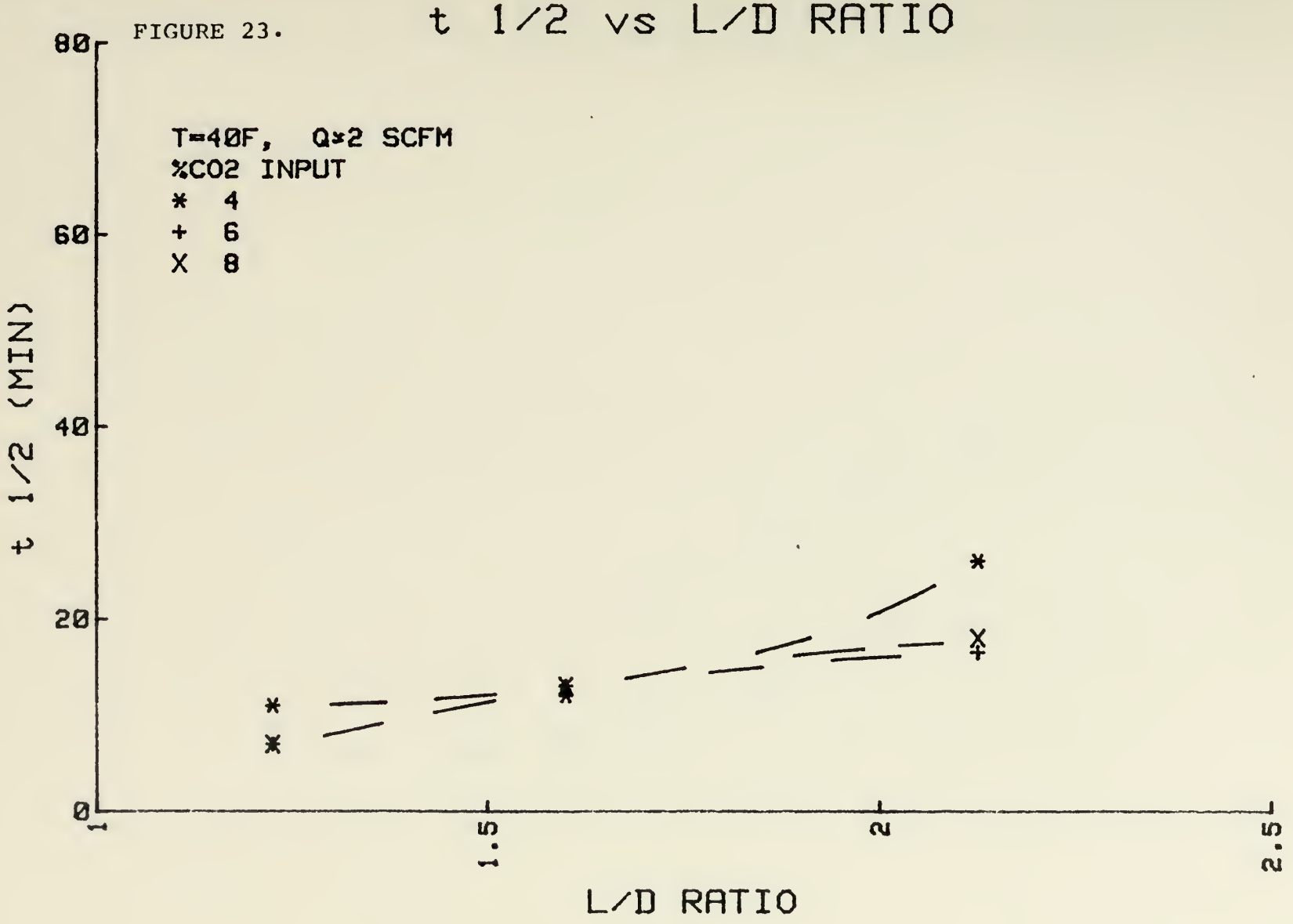
t 1/2 vs L/D RATIO
T=40F, Q=2 SCFM
%CO2 INPUT
* 4
+ 6
X 8
t 1/2 (MIN)
80
60
40
20
0
1
1.5
2
2.5
L/D RATIO

FIGURE 24.

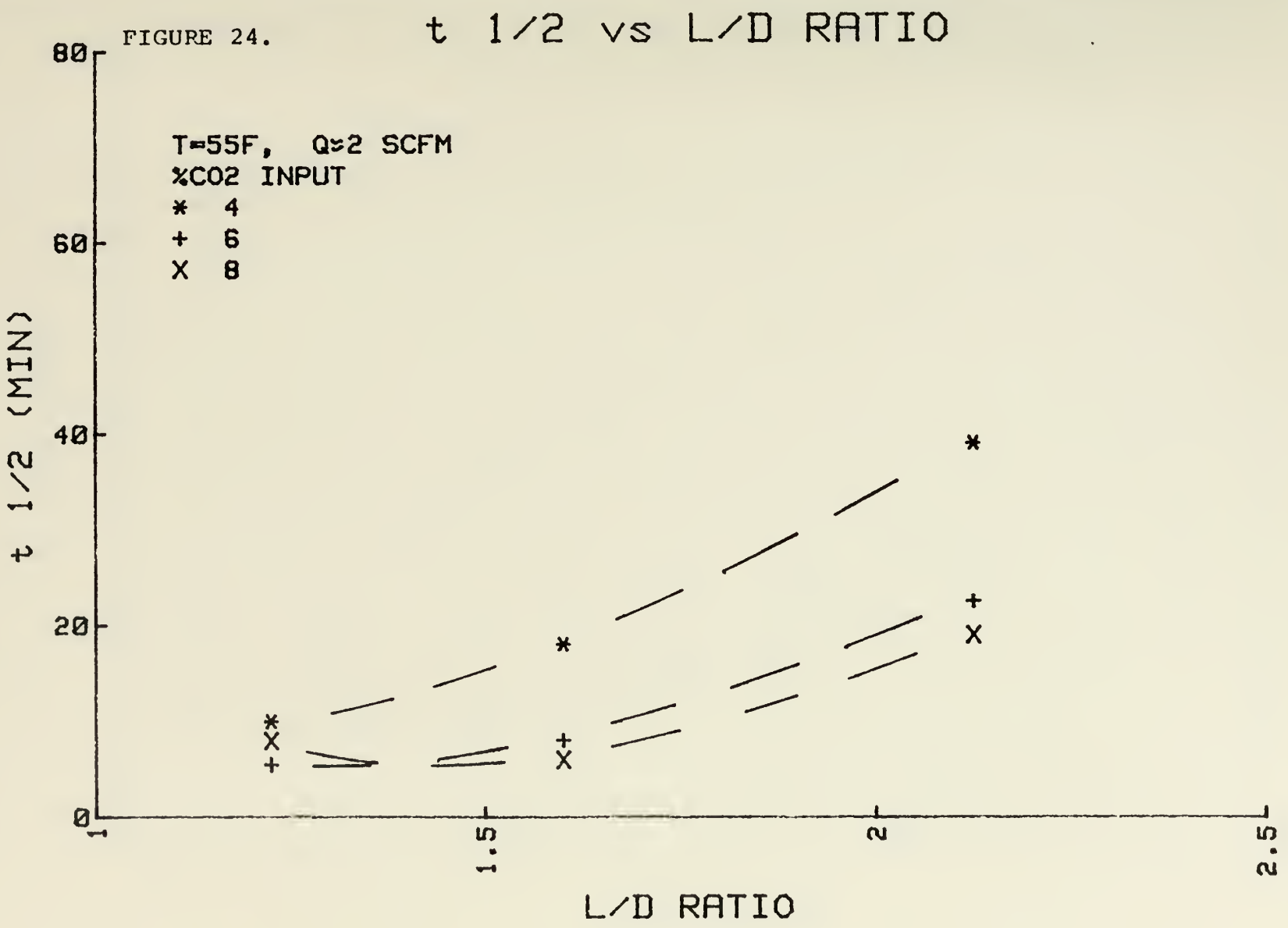
t 1/2 vs L/D RATIO
T=55F, Q=2 SCFM
%CO2 INPUT
* 4
+ 6
X 8
t 1/2 (MIN)
80
60
40
20
0
1
1.5
2
2.5
L/D RATIO

FIGURE 25.

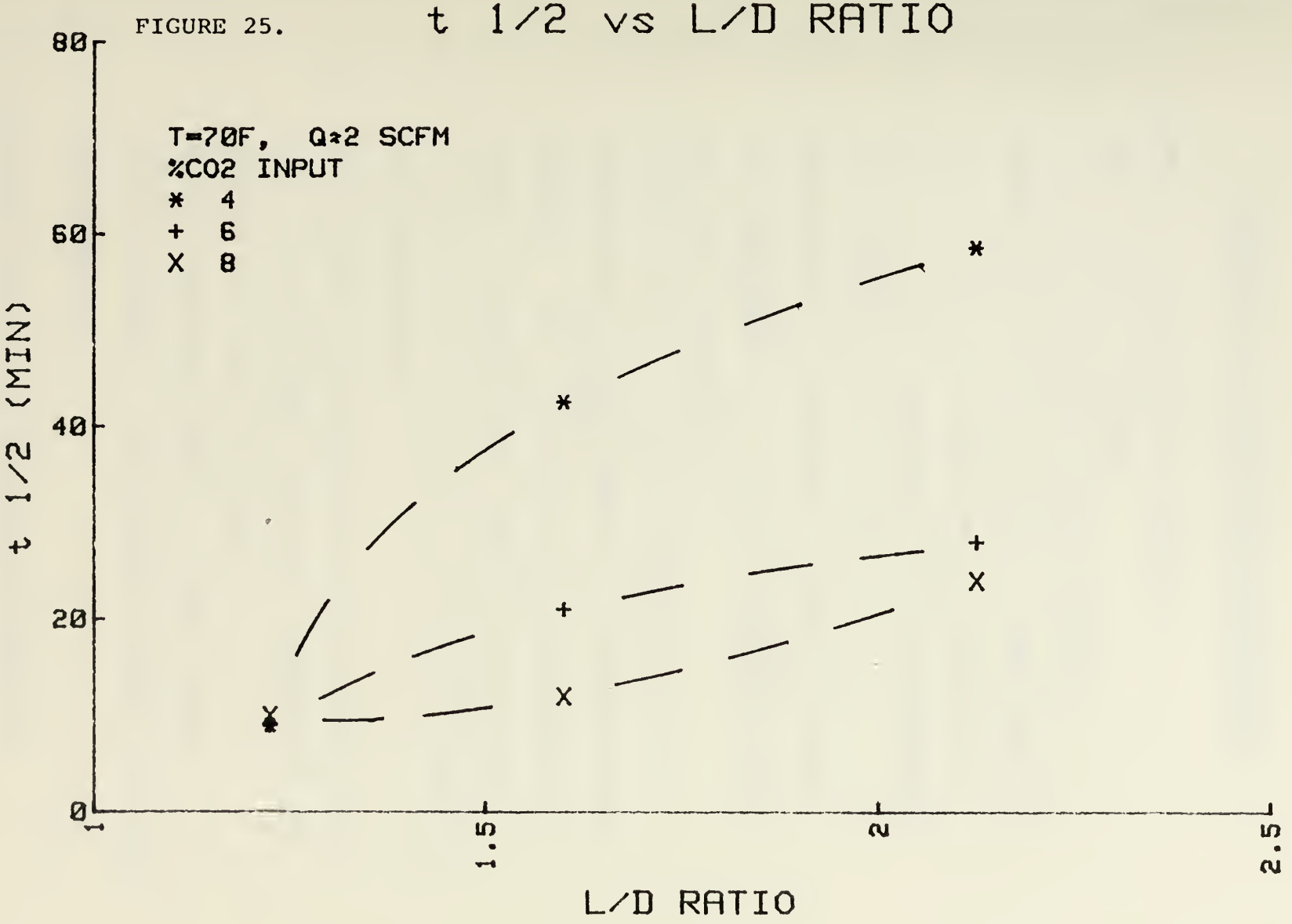
t 1/2 vs L/D RATIO
T=70F, Q=2 SCFM
%CO2 INPUT
* 4
+ 6
X 8
t 1/2 (MIN)
80
60
40
20
0
1
1.5
2
2.5
L/D RATIO

APPENDIX A: EXPERIMENTAL PROCEDURES

A. ALIGNMENT OF THE INFRARED DETECTOR

1. Warm up for 30 minutes.
2. Purge with nitrogen for five minutes.
3. RANGE to CAL, GAIN to 10XX, T A FCN switch to 100%T, SLIT to 0, check meter reading of 0.
4. SLIT to 0.5mm, WAVELENGTH to 3.5 micrometers, TIME CONSTANT to one second.
5. PATHFINDER fully counter clockwise to stops, then clockwise to 0. Adjust continuous GAIN to a meter reading of 0.6.
6. PATHFINDER fully counterclockwise to 14.26. PATHFINDER clockwise slowly to a maximum meter reading. (The PATHFINDER was consistently at 40 for a maximum meter reading on all runs.)
7. T A FCN switch to A1, SLIT to 2mm, WAVELENGTH to 4.25 micrometers.
8. By adjusting the continuous gain to read from 0 to 1.0 on the meter, align the recorder to the exact same value as the meter.
9. Adjust continuous GAIN to a meter reading of 0 while nitrogen is being purged through the infrared detector.

B. TWO HOURS PRIOR TO THE FIRST RUN OF THE DAY

1. Replace Drierite (primary and reserve) dessicant in the input line to the infrared detector.

2. Verify recorder is aligned with the infrared detector meter reading.
3. Zero all manometers.
4. Fill the water bath and constant-temperature refrigeration unit and provide a large siphon between them to assure equal water levels regardless of the flow setting on the constant-temperature refrigeration unit. Regulate the flow to maximum from the constant-temperature refrigeration unit to the water bath.
5. Drain the water separators (to the infrared detector and in the gas supply line).
6. Blow down the exhaust from the canister hose to remove any moisture.
7. Fill both humidifiers with water to 50% level.
8. Lower the temperature in the bath with ice and stabilize with constant-temperature refrigeration unit.
9. Position thermocouples at the desired lengths of the canister. Check for consistent temperature readings. Wipe out inside of the canister with ethyl alcohol and thoroughly blow dry.

C. 45 MINUTES PRIOR TO RUN

1. Shut the supply valve and open the bypass valve at the rotameter exhaust.
2. Fill the canister with fresh Sodasorb. Ensure backing screws are in a position to prevent any

movement in the Sodasorb. Horizontally inspect the canister to ensure that no movement of the Sodasorb takes place with mild shaking of the canister.

D. 30 MINUTES PRIOR TO RUN

1. Soak the canister in the water bath for 30 minutes prior to commencing the run.
2. Check the calibration of the infrared detector. (Do not continue if this is not exactly the same as the initial calibration).
3. Establish the desired supply flow rate and volume percentage of carbon dioxide. The carbon dioxide regulator and the air supply regulator should both be at ten psig. Throttle the bypass valve to produce the pressure as expected at the flowmeter in the run. Recheck the percentage of carbon dioxide with a calibrated gas. Purge the infrared detector with pure nitrogen to a meter reading of 0. Connect the output from the canister exhaust to the infrared detector. Select and record the desired recorded speed.

E. COMMENCEMENT OF RUN

1. Record start time.
2. Open the supply valve at the rotameter exhaust.
3. Shut the bypass valve at the rotameter exhaust.
4. Ensure flow to the infrared detector.

5. Do not allow moisture, dessicant dust or any greater than atmospheric pressure at the infrared detector.

F. COMPLETION OF RUN

1. Purge the infrared detector with nitrogen until the meter reads 0.
2. Check the calibration of the infrared detector at the cutoff carbon dioxide percent and the input carbon dioxide percent. (Do NOT readjust the continuous GAIN from that of the original calibration.)
3. Measure and record the input percentage of carbon dioxide.
4. Determine to the nearest half of a minute the time ($t_{1/2}$) to termination of experiment.
5. Purge the infrared detector with nitrogen.
6. Secure the supply of carbon dioxide to the canister. Continue the airflow for about five minutes.
7. Secure the air supply and remove the canister from the water bath. If upon disassembly there is any moisture or caking in the Sodasorb, repeat the entire run.
8. Clean and dry all components.
9. Replace drierite in the infrared detector supply line.

G. CONSECUTIVE RUNS

1. If consecutive runs are desired, proceed to B.5.

APPENDIX B: DATA REDUCTION RELATIONSHIPS

A. RELATIONSHIP BETWEEN AXIAL PRESSURE GRADIENT AND VELOCITY

The mass flow rate of dry nitrogen, air from the air banks and 100% humidified air was calculated using rotameter flow rate readings.

$$\dot{m} = \rho_f Q_f \quad \left(\frac{\text{lbm}}{\text{min}}\right) \tag{B1}$$

ρ_f = density of the gas at the rotameter

$$\rho_f = \frac{144 P_f}{R T_f} \quad \left(\frac{\text{lbm}}{\text{ft}^3}\right) \tag{B2}$$

P_f = absolute pressure at the rotameter (psia)

T_f = absolute temperature at the rotameter ($^{\circ}$R)

R = specific gas constant $\left(\frac{\text{ft lb}}{\text{lbm}\,^{\circ}\text{R}}\right)$

Q_f = volume per unit time of the gas passing through the rotameter $\left(\frac{\text{ft}^3}{\text{min}}\right)$

The macroscopic velocity was then calculated as

$$V_c = \frac{\dot{m}}{\rho_c A_c} \quad \text{(ft/min)} \tag{B3}$$

where:

A_c = cross sectional area of the canister (ft^2)

ρ_c = density of the gas passing through a cross section of the canister at the half length.

$$\rho_c = \frac{144\ P_{atm}}{RT_c} \qquad \left(\frac{lbm}{ft^3}\right) \tag{B4}$$

P_{atm} = absolute atmospheric pressure (psia)

T_c = approximation of the absolute temperature at a cross section of the canister at the half length

$$T_c = 460 + \frac{.875}{1.5}\left(\frac{T_4+T_{10}+T_{16}}{3}\right) + \frac{.625}{1.5}\left(\frac{T_3+T_9+T_{15}}{3}\right)(^oR) \tag{B5}$$

The axial pressure gradient was calculated by

$$(-dp/dx) \cong \frac{144\ (12)\,\Delta P_L}{27.69(8.25)} \qquad \left(\frac{lb}{ft^3}\right) \tag{B6}$$

where ΔP_L was the pressure drop across the length of the canister (inches of H_2O) and 8.25 was the length of the Sodasorb bed in the canister (inches).

The ordinate in Figure 11 was calculated as

$$\frac{1}{\mu_c V_c}\left(-\frac{dp}{dx}\right)(32.174)(60)(3600)\left(\frac{1}{ft^2}\right)$$

μ_c = absolute viscosity of the gas at T_c and atmospheric pressure. $\left(\frac{lbm}{ft\ hr}\right)$

and the abscissa was calculated from:

$$\frac{\rho_c V_c}{\mu_c} \qquad \left(\frac{1}{ft}\right)$$

The value of $1/k \left(\frac{1}{ft^2} \right)$ was then computed as the vertical intercept of Figure 11 using least-squares linear regression to minimize the sum of the squares of the deviations of the actual data points from the straight line of best fit. From this value of k, the characteristic flow dimension, $\sqrt{k}$, was determined. The slope of the line was then calculated to provide the value of b. The constant for the porous media Fanning friction value was calculated as

$$c = \sqrt{k}\, b \tag{B7}$$

The porous media Fanning friction value was calculated from

$$f = \frac{32.174(3600)\ (-\frac{dp}{dx})\ \sqrt{k}}{\rho_c V_c^2} \tag{B8}$$

and the Reynolds number was calculated by:

$$Re = \frac{60\, \rho_c V_c\, \sqrt{k}}{\mu_c} \tag{B9}$$

The Fanning friction factor, f', was then calculated from

$$f' = \frac{1}{Re} + c \tag{B10}$$

for comparison with the f calculated above.

B. THE EFFECTIVENESS OF SODASORB IN REMOVING CARBON DIOXIDE FROM AN AIR MIXTURE

Air containing 6.0% by volume carbon dioxide was passed through the porous bed media of Sodasorb at values between 1.0 and 3.8 standard cubic feet per minute. Carbon dioxide at 4.0 and 8.0% by volume was passed through Sodasorb at an approximate flow rate of two standard cubic feet per minute. The standard volumetric flow rate was calculated by:

$$Q_s = Q_f \frac{P_f}{P_s} \frac{T_s}{T_f} \qquad \left(\frac{ft^3}{min} \right) \tag{B11}$$

where:

$T_s = 530$ (^{o}R)

$P_s = 14.7$ (psia)

The volume percentage input of carbon dioxide was measured and the time ($t_{1/2}$) for 0.5% carbon dioxide by volume in the exhaust from the canister was experimentally determined.

APPENDIX C: EXPERIMENTAL UNCERTAINTY ANALYSIS

The sources of error in the results presented are due to instrument precision and accuracy, inaccuracies in geometrical measurements and uncertainty in physical constants. No attempt will be made to account for errors in assumptions such as the gas behaving as a perfect gas. The uncertainties of the final results were determined by the method of Kline and McClintock [13]. Twenty-to-one odds were used.

Instrumentation errors occurred in measuring flow rate, temperature, pressure, volume percentage of carbon dioxide in the gas and time for the exhaust gas to reach 0.5% by volume carbon dioxide. The following uncertainties were estimated:

P_{atm}:	negligible	
ΔP_L :	.5 ± .005 inches of water	± 1.0%
P_f :	15 ± .05 psia	± 0.3%
P_c :	15 ± .02 psia	± 0.1%
CO_2 :	.06 ± .001	± 1.7%
$t_{1/2}$:	30 ± .25 minutes	± 0.8%
T :	530 ± 2 ^{o}R	± 0.4%
Q_f :	2.00 ± .046 ft^3/min	± 2.3%

The flow rate (Q_f) was determined from the rotameter and compared with the turbine meter. The turbine meter was factory-calibrated in January 1979 but due to inconsistencies was factory re-calibrated in October 1979. A comparison of flow rate was then conducted in which the

turbine meter was within 6.0% of the rotameter within the central two-thirds range of the turbine meter.

The uncertainties in geometrical measurements were:

L:	6.40 ± .1 inches	± 1.6%
D:	4.00 ± .02 inches	± 0.5%

The nominal values of the gas constant (R) were obtained from Reynolds and Perkins [14] for nitrogen and air. The absolute viscosities for the gases were obtained from Vargaftik [15]. The following uncertainties were assigned:

μ:	± 1.0%
R:	± 1.0%

The characteristic flow dimension determination was not based upon single or multiple sample experiments but rather upon a least-square line fit. The uncertainty is a function of the spread, accuracy of the data points and the number of data points. This uncertainty cannot be calculated by the method of Kline and McClintock. The relative uncertainties are approximated as:

$\sqrt{k}$:	± 2.0%
b:	± 4.5%

The formula for the uncertainty in a result r which is dependent upon n independent variables is:

$$w_r = \sqrt{\left(\frac{\partial r}{\partial v_1} w_1\right)^2 + \left(\frac{\partial r}{\partial v_2} w_2\right)^2 + \ldots + \left(\frac{\partial r}{\partial v_n} w_n\right)^2} \qquad \text{(C1)}$$

where w_r is the uncertainty in the result and w_1, w_2, ... w_n are the uncertainties in the variables v_1, v_2, ...v_n.

An illustration in determining the uncertainty in the mass flow rate through the canister is demonstrated below.

$$\dot{m} = \rho_f Q_f \tag{C2}$$

$$w_{\dot{m}} = \sqrt{\left(\frac{\partial \dot{m}}{\partial \rho_f} w_{\rho_f}\right)^2 + \left(\frac{\partial \dot{m}}{\partial Q_f} w_{Q_f}\right)^2} \tag{C3}$$

$$w_{\dot{m}} = \sqrt{\left(\frac{w_{\rho_f}}{\rho_f}\right)^2 + \left(\frac{w_{Q_f}}{Q_f}\right)^2} \tag{C4}$$

The values of $\left(\frac{w_{\rho_f}}{\rho_f}\right)$ and $\left(\frac{w_{Q_f}}{Q_f}\right)$ have previously been determined as ± 1.1 and ± 2.3% respectively which results in

$$\left(\frac{w_{\dot{m}}}{\dot{m}}\right) = \pm 2.5\%$$

The uncertainties in the results based on 20:1 odds are as follows:

A_c : ± 1.0%

ρ : ± 1.1%

$\dot{m}$: ± 2.5%

V_c : ± 2.9%

-dp/dx: ± 1.9%

$\frac{1}{\mu_c V_c}\left(\frac{-dp}{dx}\right)$: ± 3.6%

$\frac{\rho_c V_c}{\mu_c}$: ± 3.3%

Re : ± 3.8%

f: ± 6.5%

c: ± 4.9%

Q_s: ± 2.4%

BIBLIOGRAPHY

1. U.S. Navy Diving Manual, Navy Department, 1970.

2. W.R. Grace & Co., Sodasorb Manual, 1962.

3. Muskat, M., The Flow Of Homogeneous Fluids Through Porous Media, J.W. Edwards, Inc., Ann Arbor, Michigan, 1946.

4. Beavers, G.S. and Sparrow, E.M., "Non-Darcy Flow Through Fibrous Porous Media," Journal Of Applied Mechanics, pp. 711-714, December 1969.

5. Scheidegger, A.E., The Physics Of Flow Through Porous Media, The MacMillan Company, New York, N.Y., 1960.

6. Ward, J.C., "Turbulent Flow In Porous Media," Journal Of The Hydraulics Division Proceedings Of The American Society Of Civil Engineers, pp. 1-12, September 1964.

7. Adriani, J., and Byrd, M.L., "A Study Of Carbon Dioxide Absorption Appliances For Anesthesia: The Canister," Anesthesiology, V. 2, pp. 450-455, 1941.

8. Conroy, W.A., and Seevers, M.H., "Studies In Carbon Dioxide Absorption," Anesthesiology, V. 4, pp. 160-173, 1943.

9. Ten Pas, R.H., Brown, E.S., and Elam, J.O.,"Carbon Dioxide Absorption, The Circle Versus The To-And-Fro," Anesthesiology, V. 19, pp. 231-239, 1958.

10. Elam, J.O., "The Design Of Circle Absorbers," Anesthesiology, V. 19, pp. 99-100, 1958.

11. Brown, E.S., "The Activity And Surface Area Of Fresh Soda Lime," Anesthesiology, V. 19, pp. 208-212, 1958.

12. Fischer and Porter Company, Specification 10A3500, Section 10A, Convertible Indicating Flowrator Meters Specification, pp. 3-5, February 1969.

13. Kline, S.J., and McClintock, F.A., "Describing Uncertainties In Single-Sample Experiments," Mechanical Engineering, pp. 3-8, January, 1953.

14. Reynolds, W.C., and Perkins, H.C., Engineering Thermodynamics, McGraw-Hill Book Co., 1977.

15. Vargaftik, N.B., Tables On The Thermophysical Properties of Liquids And Gases, 2nd ed., John Wiley and Sons, Inc., 1975.

INITIAL DISTRIBUTION LIST

	No. Copies
1. Defense Technical Information Center Cameron Station Alexandria, Virginia 22314	2
2. Library, Code 0142 Naval Postgraduate School Monterey, California 93940	2
3. Department Chairman, Code 69 Department of Mechanical Engineering Naval Postgraduate School Monterey, California 93940	2
4. Professor P.F. Pucci, Code 69Pc Department of Mechanical Engineering Naval Postgraduate School Monterey, California 93940	5
5. Systems Integration Division Diving and Salvage Department Naval Coastal Systems Laboratory Panama City, Florida 32401	2
6. Commander Naval Sea Systems Command Supervisor of Diving (Code OOC) Washington, D.C. 20350	2
7. Commanding Officer U.S. Navy Experimental Diving Unit Panama City, Florida 32401	2
8. Commanding Officer ATTN: Code 64270 Naval Air Rework Facility North Island Naval Air Station San Diego, California 92135	1
9. Commander Calvin G. Miller SMC 2531 Naval Postgraduate School Monterey, California 93940	2

Thesis 186665
M58567 Miller
c.1 The effect of flow rate and canister geometry on the effectiveness of removing carbon dioxide with soda lime.